# Alternative proteoforms and proteoform-dependent assemblies in humans and plants

Claire D. McWhite[1], Wisath Sae-Lee[2], Yaning Yuan[3], Anna L. Mallam[2], Nicolas A. Gort-Freitas[4], Silvia Ramundo[5], Masayuki Onishi[3], and Edward M. Marcotte[2]

[1]Lewis-Sigler Institute for Integrative Genomics,
Princeton University,
Princeton, NJ 08544

[2]Department of Molecular Biosciences,
The University of Texas at Austin,
Austin, TX 78712

[3]Department of Biology,
Duke University,
Durham, NC 27708

[4]Department of Systems Biology,
Harvard Medical School,
Boston, MA 02115

[5]Gregor Mendel Institute of Molecular Plant Biology
1030 Wien, Austria

Correspondence to: cmcwhite@princeton.edu

ORCIDs: C.D.M., orcid.org/0000-0001-7346-3047; W.S., orcid.org/0000-0002-0269-2851; Y.Y., orcid.org/0000-0002-4187-8157; N.A.G.-F., orcid.org/0000-0001-8614-4782; S.R., orcid/0000-0002-2703-1398; M.O., orcid.org/0000-0002-9799-4501; E.M.M., orcid.org/0000-0001-8808-180X

**ABSTRACT**

Variability of proteins at the sequence level creates an enormous potential for proteome complexity. Exploring the depths and limits of this complexity is an ongoing goal in biology. Here, we systematically survey human and plant high-throughput bottom-up native proteomics data for protein truncation variants, where substantial regions of the full-length protein are missing from an observed protein product. In humans, *Arabidopsis*, and the green alga *Chlamydomonas*, approximately one percent of observed proteins show a short form, which we can assign by comparison to RNA isoforms as either likely deriving from transcript-directed processes or limited proteolysis. While some detected protein fragments align with known splice forms and protein cleavage events, multiple examples are previously undescribed, such as our observation of fibrocystin proteolysis and nuclear translocation in a green alga. We find that truncations occur almost entirely between structured protein domains, even when short forms are derived from transcript variants. Intriguingly, multiple endogenous protein truncations of phase-separating translational proteins resemble cleaved proteoforms produced by enteroviruses during infection. Some truncated proteins are also observed in both humans and plants, suggesting that they date to the last eukaryotic common ancestor. Finally, we describe novel proteoform-specific protein complexes, where loss of a domain may accompany complex formation.

**KEYWORDS**

Proteoform, Proteolytic processing, Protein evolution, Co-fractionation / mass spectrometry (CF/MS), Alternative splicing

## INTRODUCTION

Proteoforms are protein isoforms encoded by the same gene that vary in either amino acid sequence or post-translational modification (Smith & Kelleher, 2013). One class of proteoforms is truncation variants, where an observed protein product is missing a substantial portion of its genetically encoded sequence. The full extent of protein variation in the cell is unknown (Aebersold *et al*, 2018)**,** and the number of proteins that exist as both long and short forms is similarly unknown, although many have been discovered historically**.**

Some short proteoforms are derived from alternate transcription, as in the case of the multifunctional enzyme PUR2, which is alternately transcribed as a complete tri-enzyme, or a short proteoform consisting of only its first enzyme (Henikoff *et al*, 1983). Other short proteoforms derive from post-translational limited proteolysis, as in the case of the signaling protein NOTCH1, which is proteolyzed upon activation into two short proteoforms, one that translocates to the nucleus and another that remains embedded in the cell membrane (Kopan & Ilagan, 2009). Limited/regulatory proteolysis occurs at a specific position in the protein chain, and is a distinct process from non-specific proteolytic degradation. While transcription-derived protein truncation variants may be predicted from mRNA isoforms (as for PUR2), proteoforms arising from limited post-translational proteolysis cannot easily be predicted from transcriptomes (as for NOTCH1).

Detection of a short proteoform can transform our understanding of a protein's function, as was the case with the discovery of NOTCH1's dual role as a membrane receptor and nuclear transcription factor. However, techniques that have been traditionally used to discover short proteoforms, e.g. size separation by gel electrophoresis and Western blots (Löffler & Huber, 1992), typically allow characterization of only a single protein at a time. Individual protein assays are not always easily scalable to whole proteomes, especially for species where genetic tagging is not feasible. Numerous high-throughput approaches have been developed to detect proteoforms based on "top-down" analysis of small intact proteins using mass spectrometry (e.g., as in (Dai *et al*, 2019; Ansong *et al*, 2013; Tran *et al*, 2011; Shortreed *et al*, 2016)), however these methods are roughly limited to proteoforms with a mass of less than ~50kDa. With the average mass of human protein ~62kDa, alternate methods are necessary to identify longer proteoforms at high throughput.

Alternate methods first separate proteins by size, then identify size variants by conventional "bottom-up" mass spectrometry, where proteoforms are identified by peptide coverage. For example, in the PROTOMAP approach, proteins are separated by 1D-SDS-PAGE, then gel lanes are cut into slices for protein (and associated peptide) detection (Dix *et al*, 2008). Initially used to detect proteolytic processing events based on finding N- or C-terminal short proteoforms, PROTOMAP has been broadly applied including to the discovery of short splice forms of human aminoacyl tRNA synthetases (Lo *et al*, 2014). Other notable strategies include the use of Combined Fractional Diagonal Chromatography (COFRADIC) to specifically isolate N- or C-terminal peptides (Gevaert *et al*, 2003; Staes *et al*, 2011; Van Damme *et al*, 2014; Tanco *et al*, 2017, 2017), and the related methods of COrrelation-based

functional ProteoForm (COPF) assessment and Peptide Correlation Analysis (PeCorA), in which proteoforms are detected based on the correlation among peptide abundances observed across bottom-up proteomics experiments (Bludau *et al*, 2021; Dermit *et al*, 2021).

While first denaturing proteins prior to separation allows more faithful assessment of relative sizes, in principle, retaining native interactions and protein-protein associations might allow functions of short proteoforms to be more directly interrogated. The technique of co-fractionation / mass spectrometry (CF/MS) lends itself to such an approach. CF/MS was originally designed to discover protein complexes, where cell lysate containing intact complexes is gently separated into biochemical fractions, and protein complex membership determined from protein co-elution. Complex protein mixtures can be fractionated by a variety of non-denaturing separation techniques, including size exclusion chromatography, ion exchange chromatography, isoelectric focusing, and density centrifugation. Proteins in each fraction are subsequently identified by mass spectrometry. Spurious and true interactions can be statistically evaluated and distinguished *via* machine learning based solely on experimental observations (Havugimana *et al*, 2012; Kristensen *et al*, 2012; McWhite *et al*, 2021). Importantly, buffers, detergents, and separation conditions are chosen to maximize recovery of native, endogenous protein complexes with minimal disruption.

A set of proteins that consistently co-elute across multiple different biochemical separations can be robust evidence that those proteins interact stably. Based on this principle and the corresponding freedom from specialized reagents such as recombinant tags, antibodies, or isotope labeling, CF-MS has been broadly applied to highly diverse samples in order to discover stably interacting proteins across multiple species and kingdoms of life (Havugimana *et al*, 2012; Kristensen *et al*, 2012; Wan *et al*, 2015; Aryal *et al*, 2017; McBride *et al*, 2019; McWhite *et al*, 2020; Liebeskind *et al*, 2020; Pourhaghighi *et al*, 2020; Pang *et al*, 2020; Skinnider *et al*, 2021; Skinnider & Foster, 2021). The non-denaturing conditions that preserve protein interactions can additionally protect proteins from unfolding and non-specific degradation by cellular proteases, with degradation additionally prevented by the addition of protease inhibitors to cell lysis buffers. Importantly, as CF/MS typically employs bottom-up mass spectrometry, the elution behaviors for individual (usually tryptic) peptides are recorded. This, in turn, enables their associated proteoforms to be distinguished, and in principle their native, co-eluting interaction partners to be simultaneously assayed.

Importantly, numerous CF/MS experiments spanning a variety of species are already available in the public domain to be analyzed post-hoc for truncated proteoforms, providing a rich resource for discovering new proteoforms and assessing their conservation across the tree of life. As typically conducted, CF/MS experiments are highly analogous to the standard method by which many endogenous truncated proteforms were discovered, in which proteins were separated electrophoretically and detected by e.g. Western blotting. Because truncated proteoforms are smaller than the full length protein, and tend to have distinguishable charge as well, length variants of the same protein can often be resolved on the standard separations used for CF/MS, especially size exclusion or ion exchange chromatography. **Figure 1A** depicts a typical CF/MS experiment showing such a separation of cell lysate containing the full length

form of a protein, an N-terminal fragment, and a C-terminal fragment. Based on their physical properties, these fragments elute at distinct points in the elution, and can be disambiguated by their peptide content, e.g. whether the peptides observed span the full-length protein or only sample a shorter contiguous segment, such as an N- or C-terminal fragment. Beyond allowing discovery of truncated proteins, these datasets should also allow the discovery of protein interactions between those fragments and other proteins.

Here, we surveyed elution patterns of proteins in high-throughput CF/MS fractionation experiments to detect short proteoforms that are found in high abundance, searching especially for those that do not correspond to annotated splice variants. We show that large scale bottom-up mass spectrometry can identify truncated proteoforms without limitations on longer protein length. We recover both known and novel short proteoforms in non-apoptotic human cell culture and primary red blood cells, and in two plant species, *Arabidopsis thaliana* and the single-celled green alga *Chlamydomonas reinhardtii*. We observed general trends among short proteoforms with respect to processing intrinsically disordered tails, and we identified several novel proteoforms that have been shown recombinantly to have distinct function from the full-length protein, but have not previously been shown to exist endogenously in cells. Finally, a subset of short variants are found conserved across both the human and plant lineages, suggesting that they may date to their last common ancestor 1.5 BYA or potentially older.

## RESULTS

### Co-fractionation/mass spectrometry reveals alternative proteoforms

We sought to identify short proteoforms of proteins in a systematic fashion, to determine their prevalence and evolutionary conservation, and to identify potential mechanisms for their biological production. Using the CF/MS method and taking advantage of abundant previously collected datasets as well as new ones, we developed an analytical approach to identify proteoforms with distinct sizes, charges, and peptide compositions (**Figure 1A**). By examining the elution profile for each detected tryptic peptide in a protein, and ordering these elutions from the N- to C- terminus, we can detect proteins that are shorter than their expected full length. Then, by comparing these observations to transcript isoforms, we could provide support for alternative generative mechanisms (transcription start/stop, splicing, or proteolytic (**Figure 1B**)). We specifically target limited/regulated proteolysis, and not degradative proteolysis (**Figure 1C**). As CF/MS is easily applied across species and cell types, we could additionally use a comparative proteomics approach to discern if the processing events were evolutionarily conserved.

We considered the following datasets appropriate to address this question: We selected two HEK cell size exclusion chromatography CF/MS experiments from (Mallam *et al*, 2019), one of which was treated with ribonuclease (RNAse) to help identify ribonucleoprotein complexes (**Figure 1D**), and we additionally report a new HEK cell ion exclusion chromatography CF/MS experiment. We also included four fractionations of human hemolysate, containing soluble

proteins from red blood cells (RBC) (Sae-Lee *et al*, 2022), as these cells are enucleated and do not translate protein. Therefore, protein variants in this cell type must be observed rather than inferred from mRNA isoforms. To search for conserved proteoforms, we additionally analyzed three *Arabidopsis* and three *Chlamydomonas* size and ion exchange separations from (McWhite *et al*, 2020). Overall, these data capture mass spectrometry evidence for 7,028,432 unique tryptic peptides from 13,502 proteins across 16 native biochemical fractions. **Supplemental File 1** describes features of these experiments.

As expected, the vast majority of proteins elute in a consistent manner, with peptides from the whole length of the protein found in the same biochemical fractions, which indicates that the whole protein traveled intact through the column prior to trypsin digestion to prepare the samples for mass spectrometry (**Figure 1E**). However, a small subset of observed proteins (~1%) exhibit distinctive patterns, where certain biochemical fractions contain only peptides mapping to a specific end of the protein, which indicates that multiple proteoforms existed in the lysate. These length variants can arise from alternative splicing, alternate transcriptional start/stop sites, or limited proteolysis.

**Identifying, scoring, and prioritizing candidate protein fragments**

As each CF/MS experiment measures thousands of proteins, we developed a quantitative score to prioritize proteins exhibiting alternative proteoforms. We manually assembled a validation set of proteins with suggestive peptide elution profiles, then used these cases to develop a heuristic score to prioritize proteins that may exhibit short proteoforms (**Figure 2A**).

Briefly, proteins tend to elute across chromatographic fractions in distinct peak(s) in which multiple peaks suggest the existence of proteoforms or intact proteins eluting with different binding partners. Therefore, we model protein's elution profile across the fractions as a Gaussian mixture model. Then, for each modeled peak, we consider the set of associated peptides' abundances and compute a *terminal bias* score summarizing the weight of evidence for a short proteoform eluting at that chromatographic position based on the sampling bias of peptides to either side of that position in the protein:

$$terminal\ bias = max_i(log_2\left[\left(observed_{N,i}/observable_{N,i}\right)/\left(observed_{C,i}/observable_{C,i}\right)\right]),$$

where $observed_{N,i}$ and $observed_{C,i}$ are the counts of unique peptides observed under that modeled Gaussian peak to the N- and C-terminal sides, respectively, of the potential proteoform end position *i*, and $observable_{N,i}$ and $observable_{C,i}$ are the respective counts of unique peptides to the N- and C-terminal sides of the potential end position *i* that were observed for that protein across *all* fractions. The *terminal bias* score conveys the strength of each candidate proteoform, as true truncation proteoforms will be missing observable peptides from one terminus or the other.

We evaluated the discriminatory power of the terminus bias score by assessing a withheld set of 145 proteins whose elution profiles were manually examined and found to contain one or more candidate short proteoforms. As plotted in **Figure 2B**, the score performs extremely well at prioritizing protein elution peaks corresponding to truncated proteoforms. We then verified high scoring candidate proteoforms visually, and for each proteoform added occurrences in other experiments, even if the score was below the threshold terminal bias (**Figure 2C**). The full set of proteoforms and annotated sequence coverage is provided in **Supplemental File 2**. There is a clear abundance and peptide coverage dependency in our ability to detect proteoforms. Hand-selected proteoforms were generally much more abundant than background, and score-detected proteoforms had a minimum abundance of 10 peptides. Low abundance proteoforms were only detectable if the proteoform was observed to occur at higher abundance in a different experiment (**Figure 2C)**. The number of observed proteoforms roughly correlates with sampling depth of individual experiments (**Figure 2D**). Though many proteins satisfy criteria for abundance and peptide coverage, the total number of proteins with detected short proteoforms is relatively low, ranging from 0 to 100 per fractionation experiment, where typically over 5,000 proteins are confidently identified.

Importantly, not every gap in sequence coverage corresponds to an alternative proteoform. A limitation of our approach is that multiple peptides from a protein must be observed to create robust peptide profiles. The protein must be sufficiently high in abundance, and its component peptides detected with some consistency. Our investigation of short stretches of consecutive undetected peptides (< 200 amino acids) has thus far entirely led to peptides that are poorly observable. These can correspond to hundreds of undetected amino acids flanked by regions of well-detected peptides. Many of these gaps may correspond to regions of poorly observable (non-“proteotypic”) peptides in LC/MS due to poor ionizability, or be in a region of few cleavable peptides, for example, stretches with few lysines or arginines for trypsin digestion (Mallick *et al*, 2007; Lu *et al*, 2007; Qeli *et al*, 2014), or simply not contain unique peptides, complicating their assignment in mass spectrometry reference database matching.

Nonetheless, we find that a minority of protein-coding genes produce short proteoforms that are both highly abundant and of sufficiently different size/charge variation from the long form to cause distinguishable elution behavior. The robust observations of these short proteoforms in non-apoptotic cells suggest that these short proteoforms are stably maintained.

**Short proteoform boundaries occur preferentially outside of domains**

Although pinpointing the exact start or truncation point of a short proteoform depends on peptide coverage in the mass spectrometry experiment, we observed that these positions tend to occur outside well-defined protein domains. For example, for 214 observed human proteoforms, 72% of their short proteoform boundaries fall outside protein domains (measured using InterPro (Blum *et al*, 2021a)), while these proteins are on average 54% non-domain. This finding follows the observation by Hans Neurath that limited proteolysis occurs at protein “hinges and fringes” outside of domains (Neurath, 1980).

The erythrocyte-specific proteoform of calpastatin is known to lack an N-terminal L-domain and the first of four inhibitory domains (Takano *et al*, 1986). We observe this short proteoform of calpastatin across human erythrocyte experiments, and the expected full length version in human HEK cell experiments (**Figure 3A**). Note that the y-axis does not directly scale to position along the protein; rather, it indicates consecutively ordered tryptic peptides. Interestingly, we observe an N-terminal fragment of calpastatin in erythrocytes corresponding to the lost domains of the erythrocyte-specific proteoform. This start/end point occurs between the first and second inhibitory domains.

Another particularly clear example of this apparent domain boundary trend can be seen in *Arabidopsis* beta-D-xylosidase 7 (BXL7) (**Figure 3B)**. The left (*i.e*., higher molecular weight) peak is composed of peptides from across the entire length of the protein. The right (lower molecular weight) peak contains peptides exclusively from the N-terminal glucosidase domain, and is missing all peptides from the C-terminal Ig-like fibronectin domain. Beta-D-xylosidases degrade xylan sugars, and variably contain a terminal Ig-like domain. These two proteoforms suggest that BXL7 performs dual roles, one dependent on its fibronectin extension, and one not. As the BXL7 gene has only one annotated transcript isoform (Lamesch *et al*, 2012), this event may result from proteolysis or an as yet undetermined new isoform.

Similarly, in the *Chlamydomonas* ClpP protease CLPP1, an in-frame viral DNA insertion is known to have added a long disordered tail to the encoded ClpP1 protein (Derrien *et al*, 2009), which likely extends from the assembled ClpP protease complex (**Figure 3C**). This tail is known to be proteolytically cleaved at the domain boundary to produce both heavy and light forms of the ClpP1 protein, both of which are essential (Derrien *et al*, 2009). We observe both heavy and light forms of the *Chlamydomonas* ClpP protease (**Figure 3C**). In the same way, we observe a long and short form of EIF2A in humans and *Chlamydomonas*, where the short form lacks a C-terminal coiled-coil region with no described function (**Figure 3D**).

**Alternative transcript-derived proteoforms**

By comparing truncated proteoforms' annotated mRNA transcripts, we can assign a potential source for each proteoform, *i.e.* whether it is more likely derived from a transcript variant or from limited proteolysis. 51.7% of reviewed human proteins in the Uniprot database have RNA isoform variants annotated. However, the extent to which these isoforms correspond to broadly expressed proteins is unclear (Aebersold *et al*, 2018). In our data, we find 9 truncated proteoforms in humans (out of 142 total identified) are consistent with annotated transcription variants (**Table 1**). These transcript variants derive from either alternate splicing, or alternate transcription start/stop sites. All these truncations fall between domains, suggesting that alternate splice isoforms that end mid-domain may generally not manifest into abundant protein.

For example, we observe both a full-length proteoform corresponding to the full trifunctional purine biosynthesis enzyme PUR2 (GARS-AIRS-GART) and a second N-terminal

proteoform corresponding to only the first enzyme, GARS (**Figure 4A**). A short transcript isoform of PUR2 (Henikoff *et al*, 1983) contains only the GARS enzyme and uses the same 10 exons as the full-length isoform, but is terminated by an intronic polyadenylation signal between exons 11 and 12 (Kan & Moran, 1995). We observe the trifunctional GARS-AIRS-GART and monofunctional GARS proteoforms eluting as distinct peaks.

While we initially targeted truncation variants, we do observe a clear case of a proteoform with a missing internal domain (**Figure 4B**). We observe the two major forms of Nuclear Autoantigenic Sperm Protein (NASP), the full length t-NASP and the shorter s-NASP proteoforms (Richardson *et al*, 2000). S-NASP is produced by alternate splicing of the NASP transcript, where internal exons are spliced out. An examination of the proteomic evidence for NASP confirms the presence of two proteoforms, one involving peptides from the entire NASP sequence and the second missing a large internal segment. Western blots from the Human Protein Atlas (Thul *et al*, 2017) independently confirm that both the long and short forms exist in HEK cells (**Figure 4B**). NASP is a rare example in our data of a protein with a distinct proteoform with clear internally spliced out exons, though our ability to detect this type of proteoform is highly limited by abundance and peptide coverage.

Finally, we highlight our discovery that a particular Coatomer A alternate transcript is translated into protein, and likely broadly conserved across eukaryotes. Two major proteoforms of Coatomer A are clearly distinguishable in both *Chlamydomonas* and *Arabidopsis*: a full length COPA and a novel C-terminal fragment composed of only the COPI_C domain (**Figure 4C**). Unfortunately, the protein evidence is less clear in our human samples. The observed novel short COPI_C-only protein is consistent with an mRNA isoform covering only the COPI_C domain of COPA. The isoform matching the COPI_C proteoform (A0A3B3ITI7) is only one of 13 isoforms of COPA in humans in the UniProt database (UniProt Consortium, 2019).

**Many proteoforms likely derived from proteolysis**

In the absence of already known transcript isoforms, the remainder of human truncation proteoforms likely either arise from uncharacterized mRNA isoforms or proteolysis, and potentially in some cases, a combination of both events. For example, while we observed truncated proteoforms of BTF3 and CTSC that match mRNA isoforms, these proteins also each show a second truncated proteoform that incorporates sequences not present in the known transcript isoforms (**Figure 5A-B**), suggesting that these fragments likely derive from limited proteolysis. While the C-terminal fragment of BTF3 is consistent with the isoform BTF3b, the presence of the N-terminal fragment suggests that these proteoforms derive from proteolysis (**Figure 5A**).

Though it can be difficult to prove that a proteoform does not derive from mRNA isoforms, certain proteoforms that we detect are either known to derive from proteolysis, or are similar to known proteolyzed proteins. We observe multiple cases of known limited proteolysis in our data. For example, the observed N-terminal fragment of HSD17B4 matches a fragment

produced by a known proteolysis event (**Figure 1E**) (Okumoto *et al*, 2011). We can bring to bear additional evidence from the set of proteoforms observed. In particular, when non-overlapping N- and C- terminal fragments are observed, we consider it likely that the fragments derive from cleavage. For example, human erythrocyte calpastatin exhibits non-overlapping N- and C- terminal fragments, suggesting that these fragments derive from proteolysis (**Figure 3A)**.

Endogenously, limited proteolysis is generally a regulatory event. Proteins that undergo a conformational change upon activation are natural candidates for proteolytic processing, as conformational change can expose hidden cleavage sites. For example, the protease Cathepsin is inactive until proteolysis of its N-terminal propeptide (Butler *et al*, 2019), when binding of PGRN exposes a hidden cleavage site to proteases (**Figure 5B**). We see the processed form of cathepsin in humans, *Arabidopsis*, and *Chlamydomonas*, and also capture the cathepsin propeptide in humans (**Figure 5B**).

The functional purpose of regulated proteolysis is not always so clear. Translocon at the Outer envelope membrane of Chloroplasts 159 (TOC159) contains an N-terminal highly acidic domain (A-Domain), a GTPase domain (G-domain), and a membrane anchor (M-domain). Originally thought to be a degradation product of protein extraction, the A-domain has now been shown to likely exist as an independent proteoform *in vivo*, and cleaved by an unknown protease (Agne *et al*, 2010). We observe three proteoforms of TOC159 1) the A-domain alone, 2) the A-domain with the GTPase domain, and 3) a full length proteoform in *Arabidopsis* (**Figure 5C**). For proteins known to be involved in stable complexes, short proteoforms tend to either co-elute with the same interaction partners as the full-length protein, or not co-elute. This appears to be related to macromolecular structure. The full length proteoform co-elutes with TOC75-3, another member of the TOC complex. These biochemical fractions show an enrichment for peptides from the membrane domain, potentially indicating the presence of a membrane anchor proteoform. In contrast, neither of the N-terminal short proteoforms containing the A-domain co-elute with TOC75-3. Our observation supports endogenous occurrences of both the A-domain alone, and a candidate second proteoform containing the A-domain and the GTPase domain, which both do not remain attached to the TOC complex.

Ligand binding to the NOTCH membrane receptors induces a conformational change that exposes a hidden metalloproteinase site, allowing cleavage and release of the cytoplasmic portion (Gordon *et al*, 2007). For signaling molecules, proteolysis can allow translocation of a signal after activation, such as is the case for Notch-like proteins. Fibrocystin is one such Notch-like protein in animals associated with polycystic kidney disease that is known to be first translated as a membrane protein and then proteolytically processed—probably by a proprotein convertase and ADAM metalloproteinase disintegrins—into N and C-terminal fragments that translocate away from the membrane into other compartments, with the C-terminus trafficking into the nucleus (Hiesberger *et al*, 2006; Kaimori *et al*, 2007; Follit *et al*, 2010). Similar Notch-like processing activities have not yet been characterized in green algae and plants. Nonetheless, *Chlamydomonas* has a fibrocystin/PKHD1-like ortholog (Cre07.g340450/A0A2K3DKH4) that possesses a putative signal peptide and one

transmembrane domain (Käll *et al*, 2007), has been confirmed to be N-glycosylated (Mathieu-Rivet *et al*, 2013), and thus is most likely membrane localized in a manner similar to its animal orthologs (Vagin *et al*, 2009). We observe that Cre07.g340450 exhibits short proteoforms that correspond to the mammalian ortholog's proteolytic fragments: a large N-terminal proteoform containing the transmembrane domain and the much shorter C-terminal proteoform (**Figure 5D)**. Due to the large size of the full-length protein (606 kD), we opted to validate the observed C-terminal proteoform with a recombinant tag. The mNeonGreen tagged C-terminal proteoform is indeed localized to the nucleus, supporting the occurrence of a Notch-like signaling process in *Chlamydomonas* similar to that observed in animals (**Figure 5E**).

It is important to note that no processing mechanism is yet known in the plant case, and land plants seem to lack ADAM metalloproteinase disintegrins (Blum *et al*, 2021b). However, the evolutionary conservation of the shorter proteoforms and the nuclear localization of the C-terminal construct in *Chlamydomonas* suggest the possibility that Notch-like proteolytic processing is conserved in some fashion in green algae.

**Isolated Intrinsically Disordered Termini as stable short proteoforms**

Many proteins contain an intrinsically disordered terminus (IDT) on one or both ends. Some IDTs may exert an entropic force that can shift protein conformation favorably, with a force proportional to the length of the disordered region (Keul *et al*, 2018)**.** Other IDTs modify solubility, particularly in the case of phase separated proteins (Elbaum-Garfinkle *et al*, 2015).

In contrast to our initial assumption that a lost disordered region would be immediately degraded, we detected multiple proteoforms composed entirely of a disordered terminal domain separate from the full-length protein. These IDT-only proteoforms have a consistent sequence coverage and length, suggesting regulated proteolysis or transcription, and not non-specific degradation by cellular proteases.

We detected these intact disordered termini of proteins either alone or alongside their full protein. A striking example of this can be seen with EIF3B, which is observed in its full-length form in human HEK cells, but for which we observed only the 113 amino acids of the N-terminal disordered region in RBC hemolysate (**Figure 6A**). This distinct pattern would be missed in quantification that pools observed peptides. The unique detection of the EIF3B disordered terminus alone, in the absence of the full length protein, suggests that this disorder-only proteoform is stable, long-lived (as RBCs lack transcription and translation to regenerate fresh copies of the protein), and not an artifact of sample preparation.

In contrast to the EIF3B N-terminal proteoform, which is observed in both size exclusion and ion exchange chromatographic separations, there are other disordered termini which we only observed in ion exchange experiments. For EIF3A, another member of the EIF3 complex, we observed two distinct disordered C-terminal proteoforms in both *Arabidopsis* and *Chlamydomonas* ion exchange but not size exclusion separations (**Figure 6B**). In this case, we

cannot rule out that these disordered termini were not lost during sample preparation. Regardless, they highlight the need to check if protein elution peaks contain full protein, or only portions thereof.

Most transcription factors (Liu *et al*, 2006) and many other proteins involved in regulatory control of transcription and translation (Dyson & Wright, 2005) contain at least one disordered terminus. We frequently detect at least one free disordered terminus in abundant proteins with disordered termini. For example, for both the DDX21 helicase in humans and the RH38 helicase in *Arabidopsis*, short proteoforms corresponding to independent disordered N-termini are apparent (**Figure 6C**). Other helicases we observed terminal proteoforms for are DDX6, DDX17, DDX46, DDX50, and DHX9. We additionally observed processing of multiple translation factors, including EIF4G1/2 and EIF3B in human data, IF-2 in *Arabidopsis* and *Chlamydomonas*, EIF2A in human and *Chlamydomonas* data, and EIF2B and EIF5B in all three species.

**Truncated proteoforms of translated-related proteins including EIF5B and G3BP1 resemble enterovirus infection-induced processing**

The disordered termini of numerous proteins involved in gene expression and translation also share another curious feature–they are known to be specifically cleaved by enteroviruses during infection, a modification which increases the viral load in infected cells (de Breyne *et al*, 2008). For example, viral proteolysis of the disordered terminus of EIF5B (de Breyne *et al*, 2008) causes a shift in the function of the protein, which allows increased viral replication. Interestingly, in the absence of infection, we observed endogenous proteolysis of proteins known to be cleaved by enteroviruses, including DDX6 (Saeed *et al*, 2020), HNRPM (Jagdeo *et al*, 2015), EIF5B (de Breyne *et al*, 2008), G3BP1 (Zhang *et al*, 2018), and eIF4G1/2 (Etchison *et al*, 1982). Interestingly, all these proteins are known to phase-separate (You *et al*, 2020).

**G3BP1 exhibits proteoform-specific protein interactions**

Among the enterovirus-related proteolysis events, G3BP1 is known to be cleaved by enterovirus 3C protease cleavage, leading to decreased granule formation and increased viral replication (Zhang *et al*, 2018). G3BP1 has been recently shown to act as a conformational switch (Guillén-Boixet *et al*, 2020, 1; Yang *et al*, 2020). We find a proteoform composed of the G3BP1 C -terminal RRM RNA-binding domain plus its C-terminal disordered region, which matches the proteoform produced by viral proteolysis. The remainder of the protein (*i.e.* the “other half” of our observed proteoform) has also been detected in an immunoprecipitation experiment of G3BP1 (Sanders *et al*, 2020). We observed that this short proteoform of G3BP1 tends to associate with a subset of stress granule proteins relative to the full-length G3BP1 (**Figure 7A**). This suggests that enterovirus cleavage may push G3BP1 towards a particular state favorable to the viral replication, rather than merely inactivating the protein.

**A short proteoform of USP15 interacts specifically with quinone reductase 2, TANGO2, and α-hemoglobin-stabilizing protein in red blood cells.**

In order to more systematically search for rare cases of short proteoform-specific or proteoform-enriched protein interactions such as we observed for G3BP1, we scored elution profile similarity between all pairs of proteins or protein proteoforms, looking for those that tended to occur in the same fractions over multiple experiments. The highest scoring interaction, of similar strength to the consistent co-elution of proteasome components, was an N-terminal proteoform of Ubiquitin specific protease 15 (USP15) specifically co-eluting with several other proteins: quinone reductase 2 (NQO2), Transport and Golgi organization protein 2 (TANGO2), and alpha-hemoglobin-stabilizing protein (AHSP). This interaction is strongest in red blood cell hemolysate (**Figure 7B**), though an interaction between NQO2 and Nterm-USP15 is additionally observed in our HEK experiments.

Ubiquitin specific protease 15 (USP15) is composed of three main domains: a uncharacterized domain present in ubiquitin-specific proteases (DUSP), an ubiquitin-like domain (Ubl), and a ubiquitin specific protease domain (USP). The DUSP-Ubl portion of USP15 enhances ubiquitin exchange (Clerici *et al*, 2014), and DUSP is not found in any non-USP domain architectures. Our complex contains mostly DUSP-Ubl, and little to none of the full length USP15. Though this complex is intriguing, biological interpretation of this set of interacting proteins is difficult, especially given limited knowledge of component proteins roles in red blood cells.

Nonetheless, our data support multiple proteoform generation routes, as our observed USP15 N-terminal proteoform is similar in length to an mRNA isoform, (Q9Y4E8-4), differing only by a single terminal peptide. We additionally observe a C-terminal proteoform, which does not correspond to mRNA transcripts. This suggests both a proteolytic and transcriptional route to produce the short form of USP15. Importantly, any proteoforms produced by the transcriptional route would necessarily have to be synthesized prior to red blood cell enucleation.

## DISCUSSION

### Distinguishing short proteoforms and their potential functional roles

Biochemical diversity at the mRNA-level derives mainly from alternative splicing and alternative transcription start and stop sites. While the contribution of mRNA variants to proteoform diversity is still actively being characterized and debated (Tress *et al*, 2017; Blencowe, 2017; Liu *et al*, 2017), our method does discover certain transcriptional proteoforms that substantially change charge or size characteristics of the protein. While our ability to detect these transcriptional proteoforms is dependent on high observed peptide coverage of a protein, examining the elution patterns of peptides from the N- and C-termini of proteins allows us to

detect certain highly expressed short proteoforms without the need to consider rare isoform-specific peptides.

Indeed, we observed proteoforms clearly generated by both transcript-focused and proteolytic mechanisms, and in some cases, could distinguish alternative functions attributable to the short proteoforms based on their different protein interactions, as in **Figure 7**. In general, our approach exhibits a strong bias for highly stable or abundant short proteoforms, but it seems likely that this subset of abundant, stably maintained proteoforms would more often play functional roles in cells. For example, the cleaved C-terminal domain from the Fibrocystin-like protein, Cre07.g340450, in *Chlamydomonas* can translocate into the nucleus (Figure 5D-E) while the full-length form of the protein is membrane-bound. This example shows the proteolytic process elicits cellular signals through compartmentalization of different proteoforms which in turn drives function.

There are multiple classes of protein functions where proteolysis has a functional effect beyond degradation (**Figure 8A**). For example, in the case of zymogens, proteolysis releases a terminus which physically blocks a functional site, thus activating the enzyme (Neurath & Walsh, 1976). Multifunctional proteins may be separated into their component enzymes. Proteolysis also offers a quick route to disconnect structures in the cell that are connected by linker proteins. It may also quickly release phase-separated proteins from liquid droplets, or to allow both phase-separated and non-phase-separated populations of a protein. Proteolysis can allow translocation of a signal peptide upon activation of a receptor. We find that several of our observed proteins with proteolytic fragments are known to exist as conformational switches (*e.g.* G3BP1). While these switches are reversible, proteolysis may irreversibly lock a protein in one state or another.

**Evolution of short proteoforms and proteome complexity**

Short proteoforms, whether produced by transcriptional or proteolytic processes, allow a gene to produce multiple distinct protein products, and this processing may be conserved evolutionarily. Strikingly, we observed several novel processing events to be conserved between humans and plants. These conserved short proteoforms included separation of disordered terminal domains from DDX helicases (**Figure 6C**) and other translation-related proteins. Proteolysis of signaling proteins likely often represents regulatory events. Though notch-like proteins are known to exist across plants, we demonstrate that notch-like proteolytic processing is conserved in green algae as well (**Figure 5D-E**).

Another evolutionary aspect to the production of proteoforms is that when two genes fuse, it might be expected that the original genes' individual protein products will no longer be produced, in favor of one larger fused protein (**Figure 8B**). However, generating short proteoforms of the fusion protein can result in retaining the ancestral biologically active proteins while also benefiting from the larger fused protein. Truncation of a protein has the ability to revert the protein product of a fused gene to that of one of the pre-fusion genes (Neurath, 1980). This appears to be the case for *Chlamydomonas* ClpP, which exhibits proteoforms with and without a lineage-specific extension (**Figure 3C**). Limited proteolysis or alternate transcription of

fused proteins creates an opportunity for simultaneous retention of original function and neofunctionalization, without the need for gene duplication.

**Proteoforms often vary with respect to intrinsically disordered tails**

One notable finding from our survey was that short proteoforms are enriched in certain protein families, and that certain domains are more likely to exist independently or be lost. Disordered domains were the most commonly lost domain, as for the case seen above for ClpP1 (**Figure 3C**). Intrinsically disordered tails often regulate proteins they are attached to (Uversky, 2013). Disordered regions modulate phase separation behavior (Lin *et al*, 2017), and thus are key control points.

We particularly observed candidate independent disordered domains and loss of RNA recognition motifs (RRMs) from translation-related proteins, including multiple translation factors and helicases (**Figure 6A**). Many of these proteins additionally are known to phase separate, with phase separation modulated by disordered terminal domains (Ivanov *et al*, 2019; You *et al*, 2020). Interestingly, multiple of these proteins are additionally known to be cleaved by Enteroviruses at specific positions (Saeed *et al*, 2020). We see endogenous specific proteolysis of these same translation-related proteins in human cells and plants, suggesting that Enteroviruses may mimic endogenous proteolysis events to induce a cell state that is more favorable to viral replication.

More generally, we observed numerous cases of proteoforms composed only of intrinsically disordered tails, independent from their parent proteins. Many wholly unstructured proteins perform functional roles in the cell, such as EPYC1 which mediates the phase separation of RuBisco in the algal pyrenoid body (He *et al*, 2020). It is therefore not unreasonable to suggest that intrinsically disordered domains separated from their parent protein may also have a functional purpose. While disordered termini are particularly susceptible to degradation in *in vitro* purifications, in the cell, IDTs are generally stabilized by intermolecular interactions (Suskiewicz *et al*, 2011).

While it is known that removal of disordered termini modifies protein properties, the observation of intrinsically disordered termini isolated from their parent protein suggests that some of these observed IDTs may play independent roles in the cell, rather than being immediately degraded. This is relevant to localization studies of proteins with fluorescent labels attached to disordered termini, as fluorescence may mark a truncated protein, and not exclusively the full length version. Additionally, we suggest a flag for protein data analysis for when only peptides from disordered termini are detected.

**Outside evidence of truncation proteoforms *in vivo***

It is generally challenging to prove that an observed short proteoform exists *in vivo*, and has a functional role in the cell. This is due to the possibility of non-specific proteolysis or fragmentation any time cells are lysed, as is necessary for many biochemical assays. We

suggest a series of sources of evidence for *in vivo* function of a short proteoform, whether observed from mRNA isoform, proteomic, or Western blot (**Figure 8C**), from least strong to most strong evidence. One piece of evidence would be the demonstration of individual biological function of the short proteoform, exogenously expressed. Additionally, the existence of a full-length protein corresponding to the short proteoform in either a different species or the same genome shows that the proteoform can have individual function in a cell. This follows the case of ClpP in *Chlamydomonas*, where the short proteoform of the protein matches the ClpP found in most other species (**Figure 3C**). As enteroviruses modify the cellular environment through specific proteolysis of certain proteins, endogenous proteolysis at the same sites could be expected to be functional. Next, a shift in stable protein interactions suggests that a proteoform has a distinct function from its full-length version. Additionally, if a short proteoform has distinct localization from its full-length protein, this indicates that there may be proteoform-specific transport, as in the case of Fibrocystin/Notch C-termini which are transported to the nucleus. Finally, the most rigorous evidence of a function of a specific proteolysis is to demonstrate that uncleavable variants of the protein expressed in a knock-out background cause a phenotype, or a loss of the production of the proteoform with the addition of protease inhibitors.

## CONCLUSIONS

Peptide elution profiles provide a rich and systematic source of information about native proteoforms in complex biological systems. We surveyed proteins in CF/MS proteomics experiments to detect short proteoforms that are found in high abundance, and found that roughly 1% of proteins expressed short forms. We recovered both known and novel short proteoforms in non-apoptotic human cell culture and blood and in two plant species. Many did not correspond to annotated splice variants and thus are likely to represent proteolytically generated proteoforms. A subset of short variants were found conserved across both lineages, suggesting that they may date to their last common ancestor 1.5 BYA or potentially older. We observed frequent truncation of disordered terminal domains, conserved across plants and humans. Several novel proteoforms have been shown recombinantly to have distinct function from the full-length protein, but have not previously been shown to exist endogenously in cells. We additionally demonstrated that the C-terminus of the *Chlamydomonas* ortholog of Fibrocystin/PKHD1 localizes to the nucleus, mirroring the nuclear translocation of the protealyzed Fibrocystin C-terminus in animals from the full-length membrane-localized protein. High-throughput, multispecies data from bottom-up mass spectrometry experiments thus allows the discovery and validation of conserved, abundant, stable, short proteoforms.

## METHODS

### Co-fractionation/mass spectrometry

Human HEK293T cell size exclusion CF/MS experiments were originally published in (Mallam *et al*, 2019), hemolysate CF/MS experiments were originally published in (Sae-Lee *et al*, 2021), and *Arabidopsis thaliana* and *Chlamydomonas reinhardtii* CF/MS experiments were

originally published in (McWhite *et al*, 2020), and the experiments are described in full in those publications. Previously published CF/MS experiments were retrieved from the PRIDE database (Perez-Riverol *et al*, 2019). Two additional human HEK293T cell ion exchange CF/MS experiments were collected as described in (Mallam *et al*, 2019)**,** performing ion exchange chromatography as in (McWhite *et al*, 2020). These experiments have been deposited in the Massive/ProteomeXchange protein repository and are available under accession PXD036233. **Supplemental File 1** contains Massive/ProteomeXchange accessions for all experiments.

**Protein and peptide identification**

Peptides were identified at a false discovery rate of 1% from each fraction using spectral matching algorithms MSGF+ (Kim & Pevzner, 2014), X!Tandem (Craig & Beavis, 2004), and Comet-2013020 (Eng *et al*, 2013), each run with 10ppm precursor tolerance, and allowing for fixed cysteine carbamidomethylation (+57.021464) and optional methionine oxidation (+15.9949), integrating peptide evidence across the search engines using MSBlender (Kwon *et al*, 2011). Spectra were compared to the UniProt (UniProt Consortium, 2019) human reviewed reference proteome (20,191 proteins) along with 248 common contaminants, considering up to two missed tryptic cleavages. We considered only peptides mapping uniquely to single proteins in a species (determined using the scripts trypsin.py and define_grouping.py in github.com/marcottelab/MS_grouped_lookup), and proteins with at least 10 unique peptides observed across all experiments.

**Identification of short proteoforms**

A peptide profile matrix for each protein in each experiment was created, with columns corresponding to fractions, and rows for each identified peptide. Values were peptide spectral matches, scaled from 0 to 1 across each peptide row. Initially, we generated images of each protein's peptide elutions, and hand-selected images that showed irregular elution of N- and C-terminal peptides.

Proteins elute from columns with approximately Normal/Gaussian distribution across biochemical fractions. If a protein has multiple elution points due to either protein interactions or distinct proteoforms, the protein will elute approximately with a Multivariate Gaussian distribution. To identify multiple potential individual protein elution points, we fit a Multivariate Gaussian to each protein's elution for each experiment (Figure 2A). This was done only for proteins with at least 9 unique peptides observed in an experiment. We modified the AdaptGauss R package (Ultsch *et al*, 2015) to remove the Shiny application functionality and fit up to 5 Gaussian distributions, then applied it to each protein's peptide profile to identify multiple elution peaks, if present, basing the fit of the Multivariate Gaussian on minimizing root-mean-square deviation with no penalty for additional fitted peaks. We then separated individual elution peaks using intersections between adjacent Gaussian fits of the corresponding

protein elution profile. This is a general method for segmenting multiple distinctly eluting protein species from a fractionation experiment.

To identify protein elution peaks with a skew towards either the N- or C- terminus, we calculated a terminal bias score (Figure 2A) for each elution peak composed of at least 7 unique peptides. For the peptides of each protein elution peak, a terminal bias score was calculated as described above to capture potential protein elution peaks composed of only peptides from either the N- or C-terminus of the protein. Briefly, this score captures absence of observable peptides from either end of the protein. As a manual check, proteins with high max terminal bias scores were inspected with a custom R Shiny (Chang *et al*, 2022) application, and protein elution peaks manually assigned to either full length, N-terminal, C-terminal, or internal proteoform categories.

For the case of human proteins, we compared the resulting proteoforms' sequence coverage to mRNA isoforms annotated in the Uniprot human reference proteome. We considered our proteoforms to be potentially derived from an mRNA isoform with a highly permissive criterion, specifically if the observed proteoform overlapped at least 50% the expected length of the expected mRNA isoform protein product.

All code and data analysis are available from https://github.com/marcottelab/peptide_elutions/

**Plasmid construction, *Chlamydomonas* transformation, and microscopy**

pYY025 ($P_{PSAD}$*:PKHD1_C_Ter-CrNeonGreen-3FLAG:APHVIII*) was constructed by isothermal recombination reaction (Gibson *et al*, 2009) of two fragments: (a) A DNA sequence encoding *Chlamydomonas* fibrocystin C-terminus (amino-acid positions 4415-4952), amplified from genomic DNA of wild-type strain CC-124 using the following primers: F: 5'-ATTTGCAGGAGATTCGAGGTTATGCGCGCCGCCGCCAAGCGCCGC -3', R: 5'-CCTCGCCCTTGGACACCATGTTGTTGGCGTGGCGCTGGCGCATGCTGT-3' (1660 bps) and KOD Xtreme Hot Start DNA Polymerase (Toyobo, Cat No. 71975). (b) A bicistronic-mRNA-based expression vector pMO666 ($P_{PSAD}$*:CrNeonGreen-3FLAG:APHVIII*) digested with HpaI (Onishi and Pringle, 2016).

pYY025 was linearized using ScaI and transformed into wild-type strain CC-124 by electroporation as previously described (Onishi & Pringle, 2016), except that concentration of paromomycin (RPI, Cat No. P11000) used for selection was reduced to 5 µg/ml.

Cells of positive transformants were cultured in 5 ml liquid Tris-acetate-phosphate (TAP) medium in a 100 ml glass jar at room temperature under constant illumination at 50-70 µmol photons $\cdot$ $m^{-2} \cdot s^{-1}$ for 2 days. Cells were mounted on glass slides with liquid TAP medium. Images were taken with a Leica Thunder Cell Culture inverted microscope equipped with an HC PL APO 63X/1.40 N.A. oil-immersion objective lens. Signals were captured using the following excitation and emission wavelengths: 510 nm and 535/15 nm for mNeonGreen; 640 nm and 705/72 nm for chlorophyll autofluorescence. Fluorescence images were captured with 0.41 µm

Z-spacing covering the entire cell volume; resulting images were processed through deconvolution and maximum-projected.

## Conflicts of interest

The authors declare no conflicts of interest.

## Funding

CDM acknowledges support from the Lewis-Sigler Institute for Integrative Genomics and NIH (F31 GM12384856). EMM acknowledges support from the Welch Foundation (F-1515), Army Research Office (W911NF-12-1-0390), and NIH (R35 GM122480, R01 HD085901). MO acknowledges partial support from NSF (MCB-1818383). The authors thank the Texas Advanced Computing Center at The University of Texas at Austin for providing high-performance computing resources that have contributed to the research results reported in this paper.

**Table 1:** Correspondence of observed short proteoforms with known human isoforms. Observed coverage for N-terminal proteoforms spans from the N-terminus to the last observed amino acid. Observed coverage for C-terminal proteoforms spans from the first observed amino acid to the C-terminus.

| ProteinID | Term | Observed coverage | Isoform coverage | Uniprot Isoform ID | Observed experiments |
|---|---|---|---|---|---|
| sp\|P22307\|NLTP_HUMAN | C | 405-547 | 405-547 | SCP2 | HEK_SEC2, HEKR_SEC2 |
| sp\|P22102\| _HUMAN | N | 5-433 | 1-433 | Short | HEK_IEX1, HEK_IEX2, HEK_SEC1, HEK_SEC2, HEKR_SEC1 |
| sp\|Q5JSH3\|WDR44_HUMAN | C | 525-886 | 474-913 | 3 | HEK_IEX1 |
| sp\|P20290\|BTF3_HUMAN | C | 80-206 | 45-206 | 2 | HEK_IEX1, HEKR_SEC1 |
| sp\|P46108\|CRK_HUMAN | N | 21-179 | 1-204 | Crk-I | HEMO_IEX1, HEMO_IEX2, HEMO_SEC1, HEMO_SEC2 |
| sp\|P35249\|RFC4_HUMAN | N | 7-232 | 1-303 | 2 | HEK_IEX2, HEK_SEC1 |
| sp\|Q4VCS5\|AMOT_HUMAN | C | 413-856 | 410-1084 | 2 | HEK_IEX1, HEK_SEC1, HEKR_SEC1 |
| sp\|Q71RC2\|LARP4_HUMAN | N | 139-428 | 1-445 | 7 | HEKR_SEC1 |
| sp\|A0MZ66\|SHOT1_HUMAN | C | 467-593 | 413-631 | 7 | HEK_IEX2 |

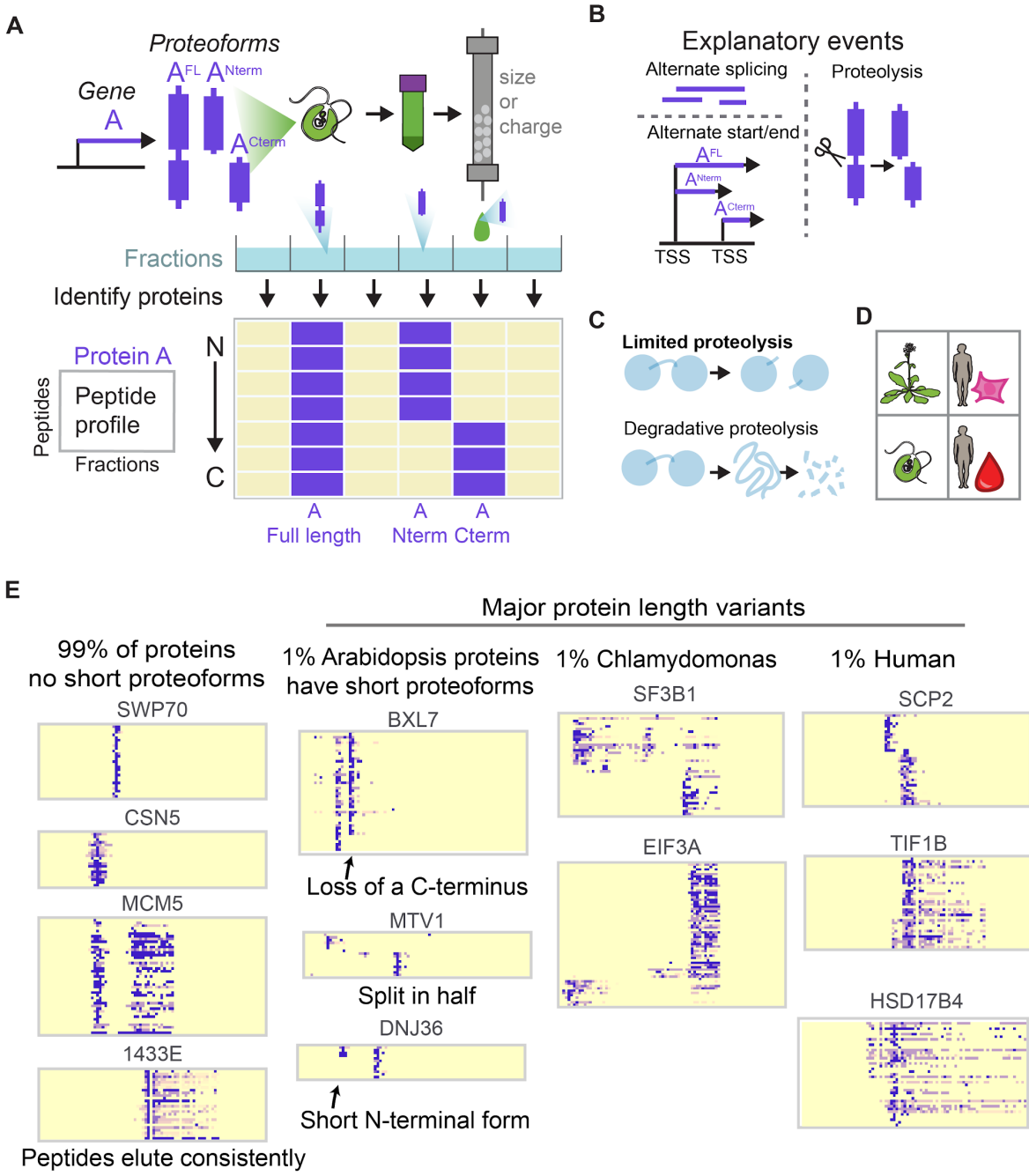
A
Proteoforms
Gene
A
AFL ANterm
ACterm
size
or
charge
Fractions
Identify proteins
Protein A
Peptides
Peptide
profile
Fractions
N
C
A
Full length
A
Nterm
A
Cterm
B
Explanatory events
Alternate splicing
Proteolysis
Alternate start/end
AFL
ANterm
ACterm
TSS
TSS
C
Limited proteolysis
Degradative proteolysis
D
E
Major protein length variants
99% of proteins
no short proteoforms
1% Arabidopsis proteins
have short proteoforms
1% Chlamydomonas
1% Human
SWP70
CSN5
MCM5
1433E
Peptides elute consistently
BXL7
Loss of a C-terminus
MTV1
Split in half
DNJ36
Short N-terminal form
SF3B1
EIF3A
SCP2
TIF1B
HSD17B4

**Figure 1. Alternative proteoforms are evident in an examination of peptide elution profiles from co-fractionation / mass spectrometry experiments.**

(A) One gene can produce multiple proteoforms. To detect these proteoforms, cells are lysed, and the native lysate biochemically fractionated by e.g. ion exchange or size exclusion chromatography, with proteins in each fraction subsequently identified and quantified by protein mass spectrometry. Distinct proteoforms can be visualized and identified by plotting the elution patterns of individual peptides ordered from the N- to the C- terminus. A full length protein has peptides covering the whole sequence of the protein, while truncated proteoforms will only have peptides from one terminus. These proteoforms can derive from alternate splicing, alternate start/end transcription sites, or proteolysis.

(B) Truncated peptides can be derived from alternative splicing, proteolysis, and alternative start/end points on mRNA.

(C) Limited proteolysis involves a specific cleavage point in the protein chain, in contrast to non-specific degradative proteolysis.

(D) Species and samples analyzed in this study.

(E) While a large majority of proteins show only a single full-length proteoform in these datasets, roughly 1% of proteins exhibit additional, shorter proteoforms.

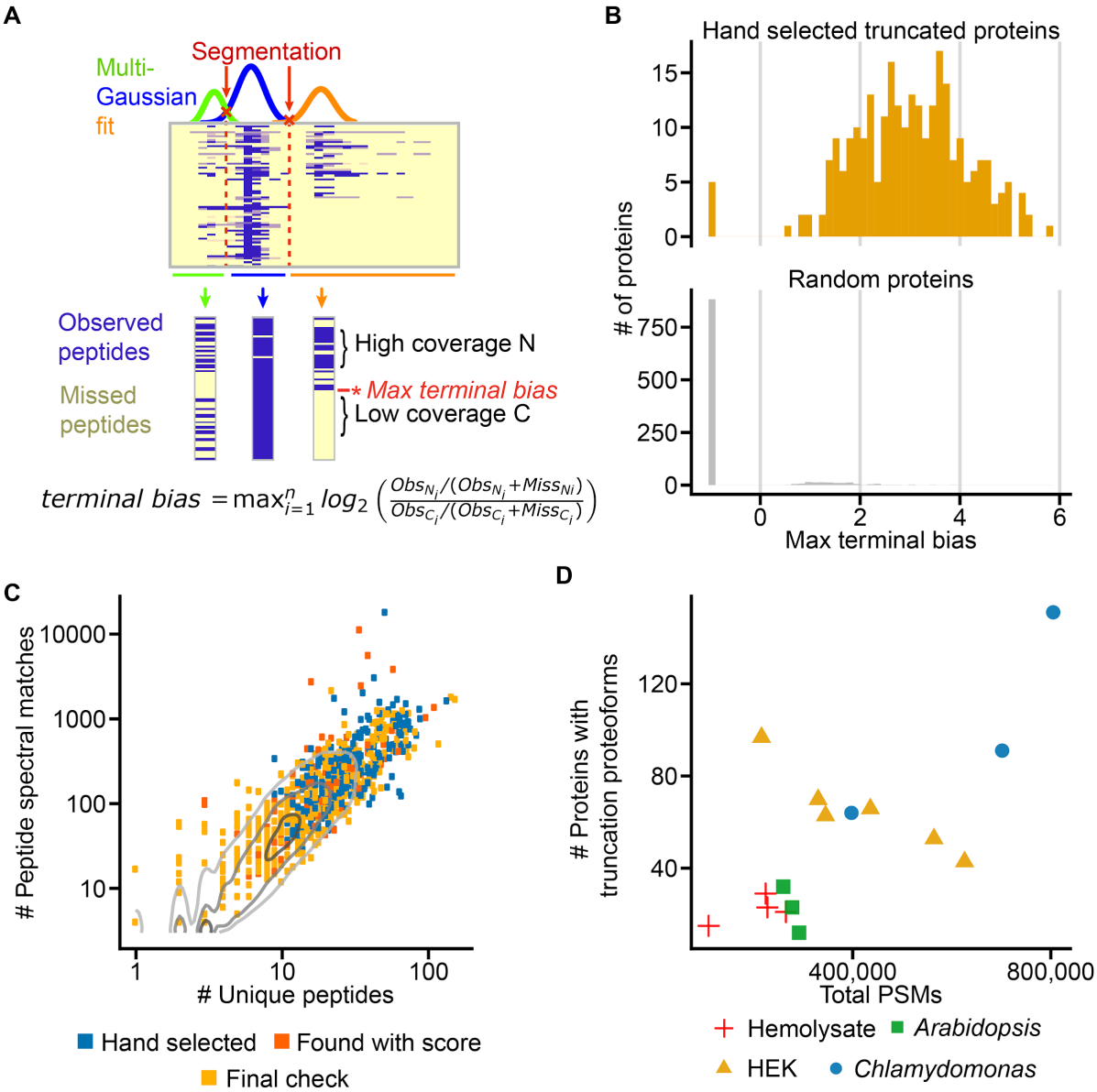
A
Segmentation
Multi-
Gaussian
fit
Observed
peptides
Missed
peptides
High coverage N
Max terminal bias
Low coverage C
$terminal\ bias = \max_{i=1}^{n} log_2 \left( \frac{Obs_{N_i}/(Obs_{N_i}+Miss_{Ni})}{Obs_{C_i}/(Obs_{C_i}+Miss_{C_i})} \right)$
B
Hand selected truncated proteins
Random proteins
# of proteins
Max terminal bias
C
# Peptide spectral matches
# Unique peptides
Hand selected
Found with score
Final check
D
# Proteins with
truncation proteoforms
Total PSMs
Hemolysate
Arabidopsis
HEK
Chlamydomonas

**Figure 2. Automating detection of alternative proteoforms in plant and human CF/MS experiments.**

(A) Multiple gaussians are fit to a protein's peptide elution profile. The intersections of these gaussians are used to segment the elution profile. For each segment, we calculate a terminal bias at each peptide. For each protein, we save the maximum terminal bias, which corresponds to the start or truncation point of a proteoform.

(B) Proteins with apparent short proteoforms have higher max terminal bias scores than randomly selected proteins.

(C) Compared to the background distribution of unique peptides per protein and peptide spectral matches, proteins for which we are able to detect proteoforms are relatively abundant. The terminal bias score prioritizes some proteins with lower abundance than our hand-selected proteoforms. In a final visual check, for some experiments, we identified a short proteoform at low abundance if the same protein had a more confident proteoform in a different experiment.

(D) Number of proteoforms identified per experiment depends on the number of unique peptides identified in the experiment.

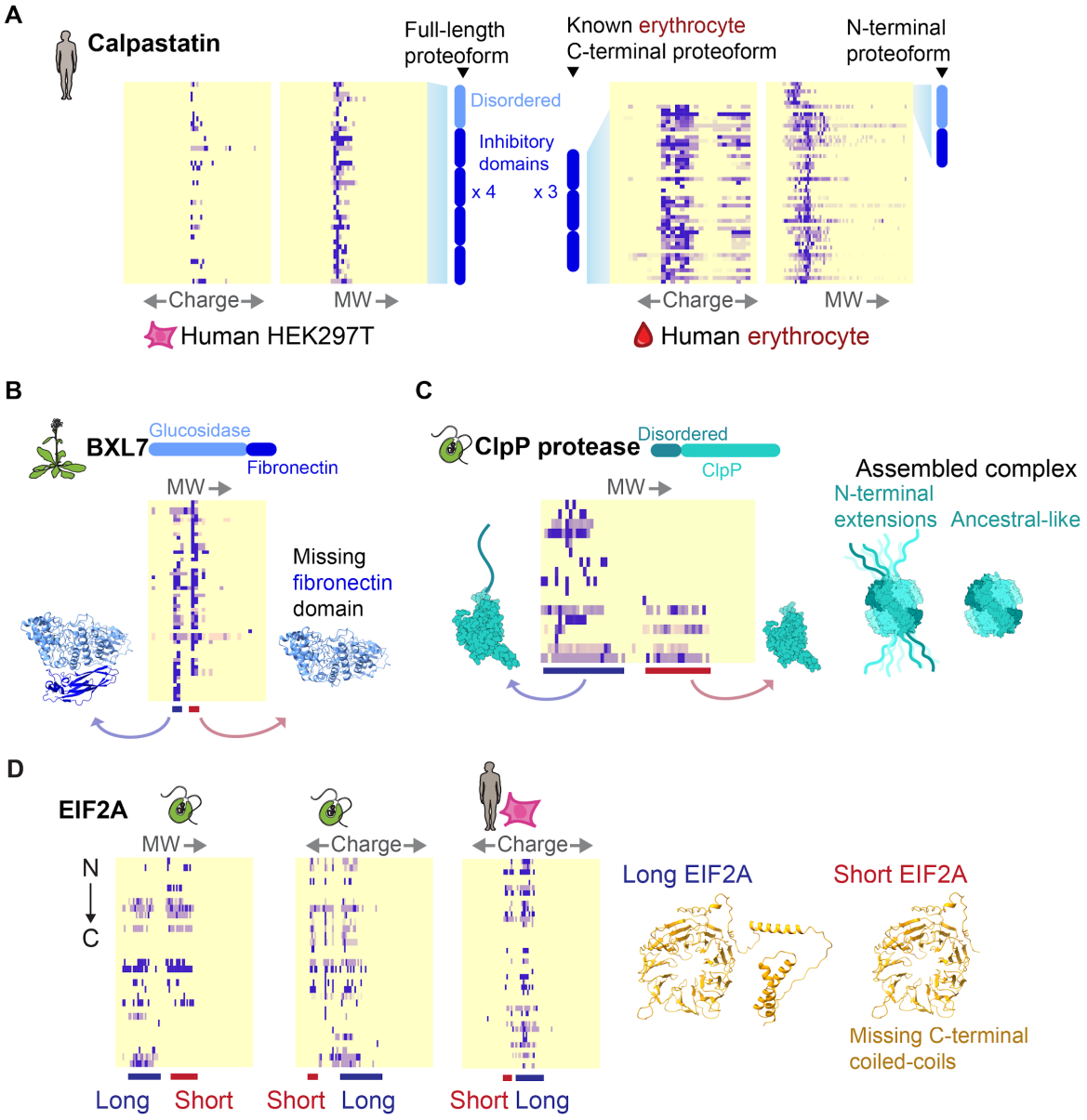
A
Calpastatin
Full-length proteoform
Known erythrocyte C-terminal proteoform
N-terminal proteoform
Disordered
Inhibitory domains
x 4
x 3
Charge
MW
Charge
MW
Human HEK297T
Human erythrocyte
B
BXL7
Glucosidase
Fibronectin
MW
Missing fibronectin domain
C
ClpP protease
Disordered
ClpP
MW
Assembled complex
N-terminal extensions
Ancestral-like
D
EIF2A
MW
Charge
Charge
N
C
Long
Short
Short
Long
Short
Long
Long EIF2A
Short EIF2A
Missing C-terminal coiled-coils

**Figure 3. Short proteoform boundaries occur preferentially outside of domains.**

(A) Cell-type specific proteforms of calpastatin. In HEK293T cells, we observe a full length proteoform of calpastatin containing all domains, while in erythrocytes we observe the erythrocyte-specific proteoform containing only the final three inhibitory domains. Unexpectedly, we observe an N-terminal proteoform of calpastatin in erythrocytes.

(B) In *Arabidopsis* we observe two proteoforms of BXL7, one with, and one without the c-terminal fibronectin domain.

(C) In *Chlamydomonas*, we observe two forms of the ClpP protease, one with, and one without an essential N-terminal disordered extension.

(D) In *Chlamydomonas,* and potentially humans, we observe a form of EIF2A with and without C-terminal alpha coils.

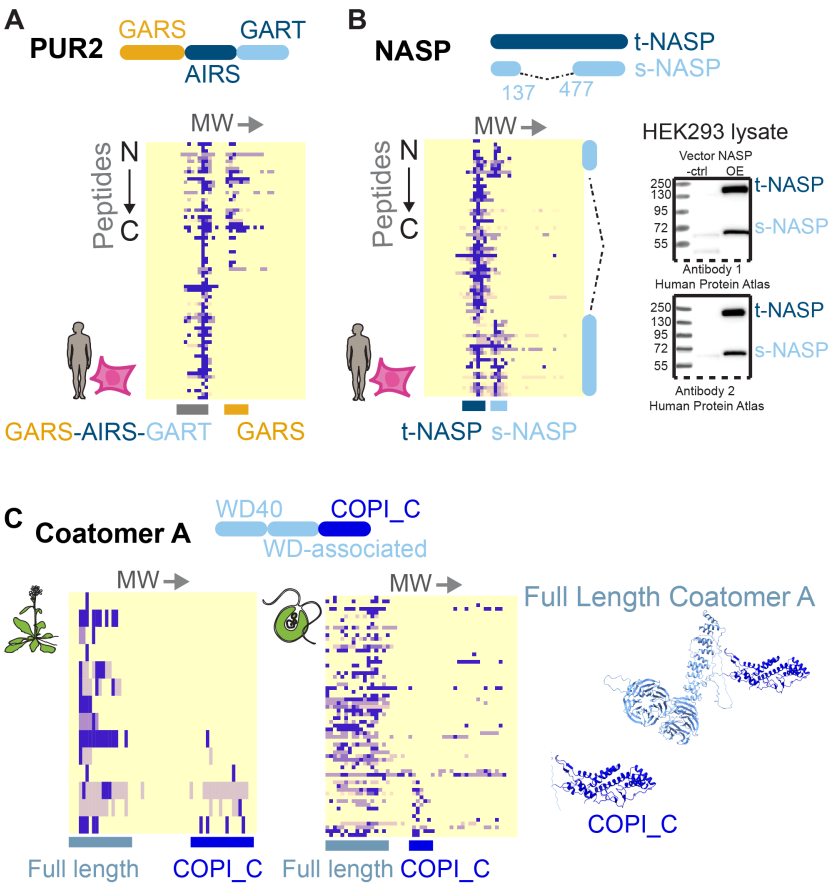


**Figure 4. Known and novel transcript-directed generation of short proteoforms.**

A) The *GART* gene encodes both a tri-functional enzyme GARS-AIRS-GART and the mono-enzyme GARS. The short form derives from an early transcription stop site. We detect both forms.

B) Two known proteoforms of NASP, t-NASP and s-NASP are detected in HEK293T elutions. The same proteoforms are detected with two independent antibodies in the Human Protein Atlas(V21). Images available at http://www.proteinatlas.org/ENSG00000132780-NASP/antibody

C) Two major proteoforms are evident for the Coatomer A protein from *Chlamydomonas*, a full length COPA and a C-terminal proteoform composed of only the COPI_C domain, consistent with mRNA isoforms corresponding to this novel short protein being found broadly across eukaryotes.

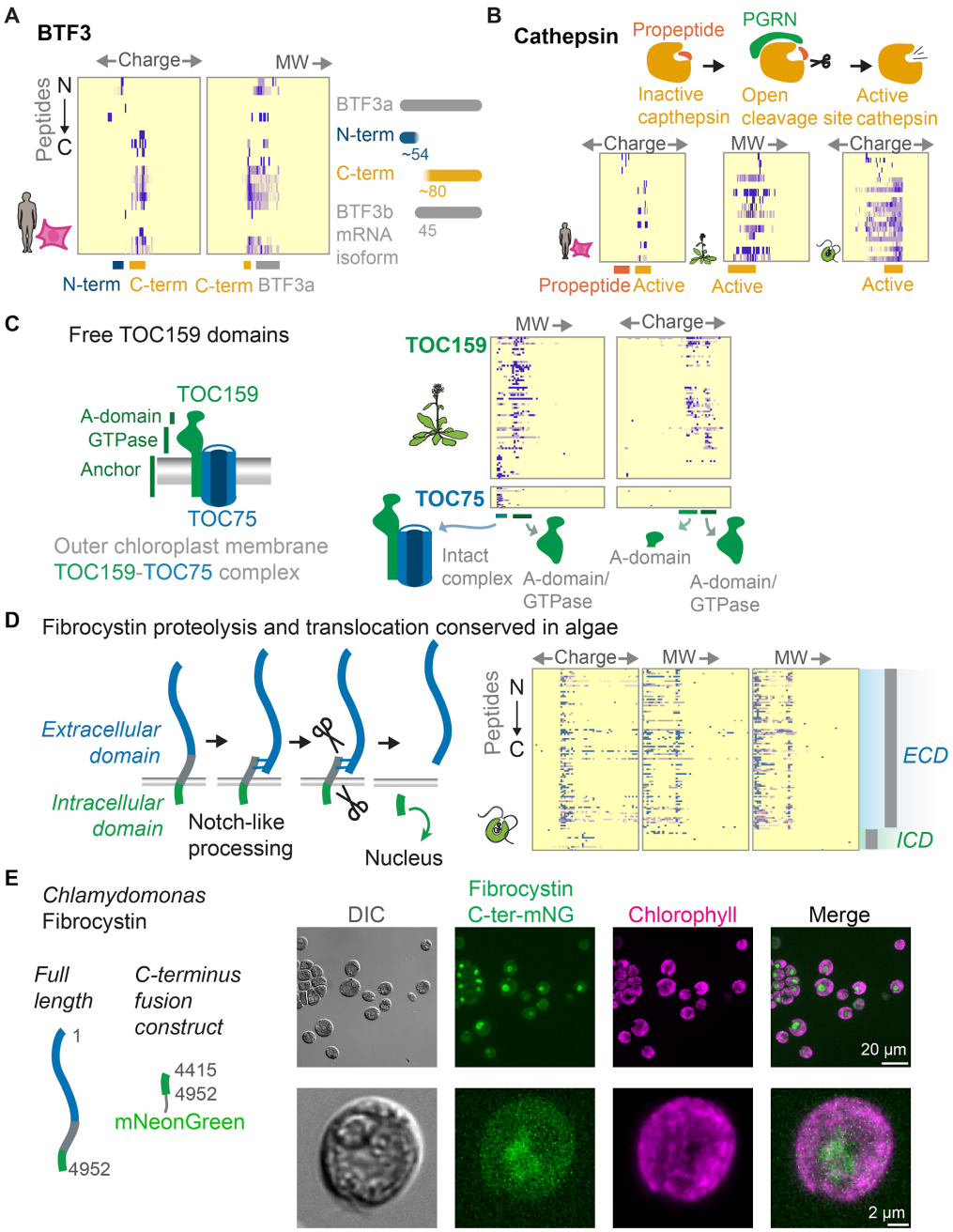


**Figure 5. Numerous proteoforms likely derive from proteolysis.**

(A) In humans, we observe N- and C-terminal proteoforms for the transcription factor BTF3. While a C-terminal mRNA isoform exists, the presence of the N-terminal proteoform suggests that these proteoforms derive from proteolysis.

(B) In humans, *Arabidopsis*, and *Chlamydomonas* we observe activated cathepsin, where the N-terminal propeptide has been removed by the interaction with PGRM. In humans, we observe the propeptide alone along with the activated form.

(C) TOC proteins form a complex at the chloroplast membrane. We observe TOC159 in three forms, one full length proteoform in complex with the TOC membrane anchor TOC75, one N-terminal proteoform containing the A-domain and the GTPase, and one N-terminal proteoform containing only the A-domain. Neither of the N-terminal proteoforms co-elute with TOC75 showing that these proteoforms have disassociated from the rest of the TOC complex.

(D-E) Fibrocystin/PKHD1 undergoes proteolysis at two positions, one in the N-terminal extracellular domain, which undergoes NOTCH-like cleavage, and one at the intracellular C-terminal domain which releases the C-terminus to go to the nucleus. While this processing is known in animals, it was not known to occur in green algae, but the observed proteoforms (at right) support fibrocystin cleavage in *Chlamydomonas* . (E) A *Chlamydomonas* fibrocystin C-terminal proteoform can localize to the nucleus. Truncated fibrocystin sequence (amino-acid positions 4415-4952) fused to mNeonGreen was expressed from the constitutive *PSAD* promoter.

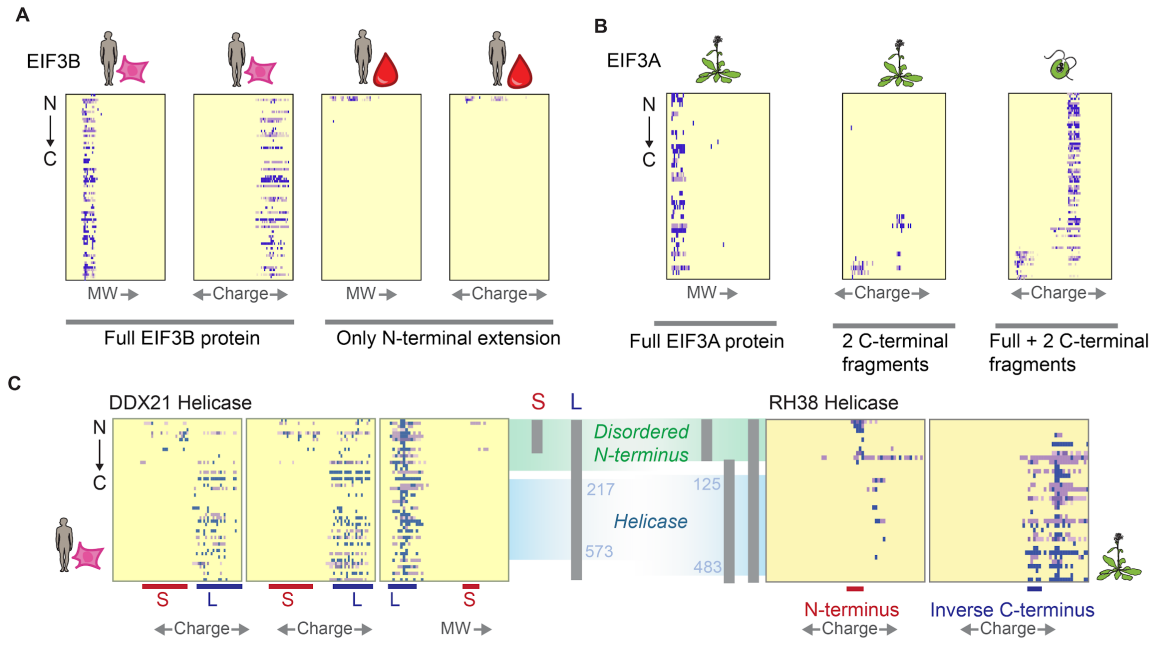


**Figure 6. Numerous endogenous proteins exhibit loss of a disordered terminus corresponding to known enterovirus cleavage events.**

(A) While in HEK293 cells, we observe full length EIF3B, in erythrocytes we only observe peptides from its short N-terminal disordered region.

(B) We observe various C-terminal proteoforms of EIF3A in *Arabidopsis* and *Chlamydomonas*

(C) For proteins with a disordered terminus, we frequently observe either independent proteoforms of just the disordered portion, or loss of disordered termini.

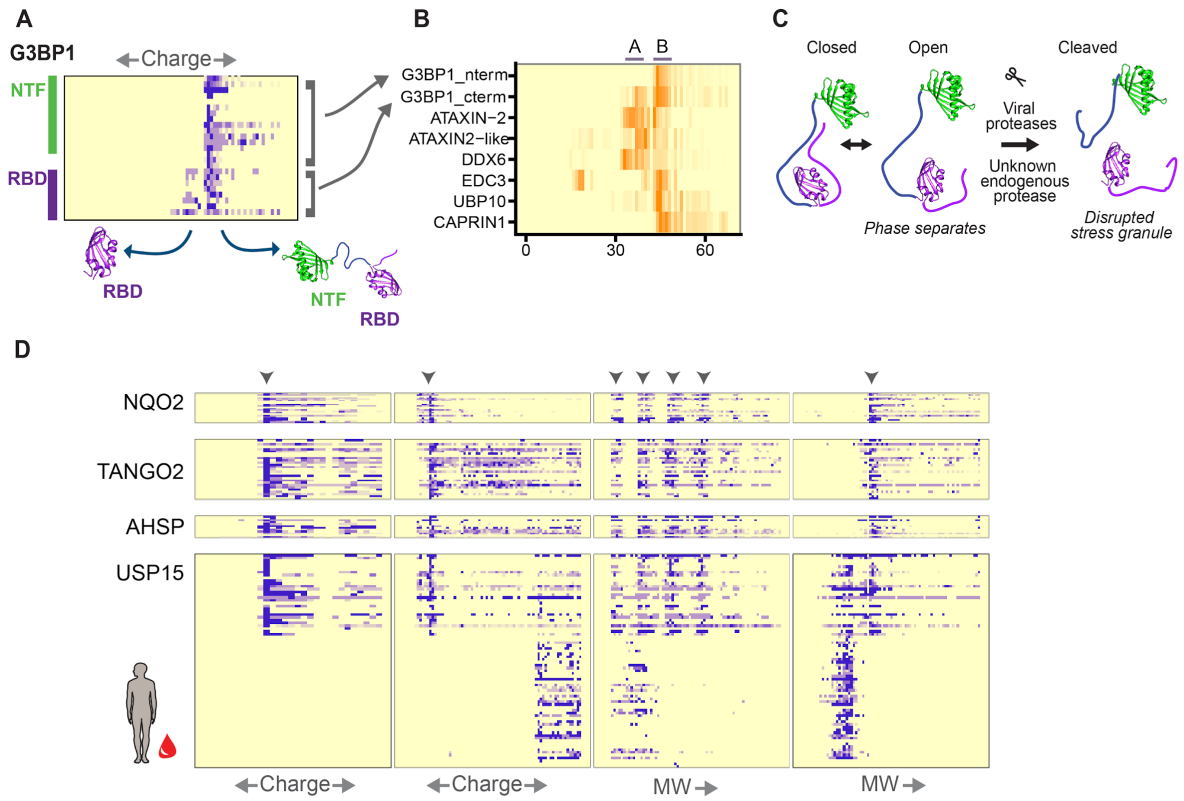


**Figure 7. Proteoform-specific protein interactions**

(A) We observe both full-length and C-terminal RBD domain-only proteoforms of G3BP1.

(B) The C-terminus of G3BP1 is enriched for interactions with ATAXIN2, ATAXIN2-like, and DDX6 proteins, relative to full length G3BP1.

(C) G3BP1 has open and closed conformations. Viral proteases cleave G3BP1, disrupting stress granule formation. An unknown endogenous protease may additionally disrupt stress granule formation via proteolysis of G3BP1.

(D) We observe a protein complex of NQO2, TANGO2, AHSP, and the N-terminus of USP15 in erythrocytes. The C-terminus of USP15 and the full length form of USP15 are not involved in the complex.

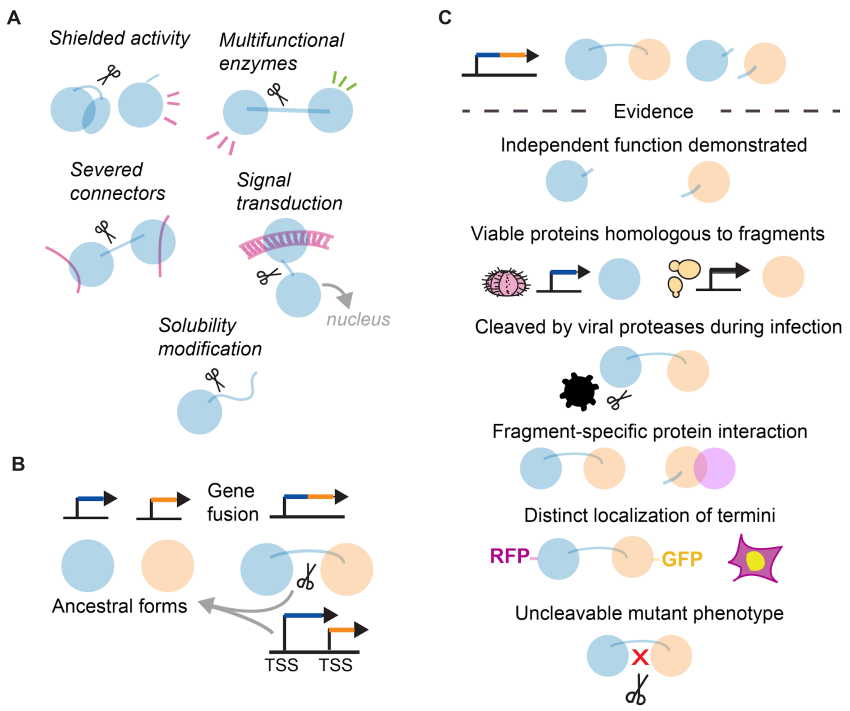


**Figure 8. Diverse modes of short proteoform generation and cellular function and evidence.**

(A) Proteolysis can play numerous functional roles beyond degradation in generating short proteoforms.

(B) For the case of fusion proteins, the generation of short proteoforms may serve to re-create ancestral protein functionality while also benefiting from the larger fused protein.

(C) Varying lines of evidence are suitable for learning the *in vivo* functions of a short proteoform.

**References**


Aebersold R, Agar JN, Amster IJ, Baker MS, Bertozzi CR, Boja ES, Costello CE, Cravatt BF, Fenselau C, Garcia BA, *et al* (2018) How many human proteoforms are there? *Nat Chem Biol* 14: 206–214

Agne B, Andrès C, Montandon C, Christ B, Ertan A, Jung F, Infanger S, Bischof S, Baginsky S & Kessler F (2010) The Acidic A-Domain of Arabidopsis Toc159 Occurs as a Hyperphosphorylated Protein1[W][OA]. *Plant Physiol* 153: 1016–1030

Ansong C, Wu S, Meng D, Liu X, Brewer HM, Kaiser BLD, Nakayasu ES, Cort JR, Pevzner P, Smith RD, *et al* (2013) Top-down proteomics reveals a unique protein S-thiolation switch in Salmonella Typhimurium in response to infection-like conditions. *Proc Natl Acad Sci* 110: 10153–10158

Aryal UK, McBride Z, Chen D, Xie J & Szymanski DB (2017) Analysis of protein complexes in Arabidopsis leaves using size exclusion chromatography and label-free protein correlation profiling. *J Proteomics* 166: 8–18

Blencowe BJ (2017) The Relationship between Alternative Splicing and Proteomic Complexity. *Trends Biochem Sci* 42: 407–408

Bludau I, Frank M, Dörig C, Cai Y, Heusel M, Rosenberger G, Picotti P, Collins BC, Röst H & Aebersold R (2021) Systematic detection of functional proteoform groups from bottom-up proteomic datasets. *Nat Commun* 12: 3810

Blum M, Chang H-Y, Chuguransky S, Grego T, Kandasaamy S, Mitchell A, Nuka G, Paysan-Lafosse T, Qureshi M, Raj S, *et al* (2021a) The InterPro protein families and domains database: 20 years on. *Nucleic Acids Res* 49: D344–D354

Blum M, Chang H-Y, Chuguransky S, Grego T, Kandasaamy S, Mitchell A, Nuka G, Paysan-Lafosse T, Qureshi M, Raj S, *et al* (2021b) The InterPro protein families and domains database: 20 years on. *Nucleic Acids Res* 49: D344–D354

de Breyne S, Bonderoff JM, Chumakov KM, Lloyd RE & Hellen CUT (2008) Cleavage of eukaryotic initiation factor eIF5B by enterovirus 3C proteases. *Virology* 378: 118–122

Butler VJ, Cortopassi WA, Argouarch AR, Ivry SL, Craik CS, Jacobson MP & Kao AW (2019) Progranulin Stimulates the In Vitro Maturation of Pro-Cathepsin D at Acidic pH. *J Mol Biol* 431: 1038–1047

Chang W, Cheng J, Allaire JJ, Sievert C, Schloerke B, Xie Y, Allen J, McPherson J, Dipert A & Borges B (2022) shiny: Web Application Framework for R

Clerici M, Luna-Vargas MPA, Faesen AC & Sixma TK (2014) The DUSP–Ubl domain of USP4 enhances its catalytic efficiency by promoting ubiquitin exchange. *Nat Commun* 5: 5399

Craig R & Beavis RC (2004) TANDEM: matching proteins with tandem mass spectra. *Bioinforma Oxf Engl* 20: 1466–1467

Dai Y, Buxton KE, Schaffer LV, Miller RM, Millikin RJ, Scalf M, Frey BL, Shortreed MR & Smith LM (2019) Constructing Human Proteoform Families Using Intact-Mass and Top-Down Proteomics with a Multi-Protease Global Post-Translational Modification Discovery Database. *J Proteome Res* 18: 3671–3680

Dermit M, Peters-Clarke TM, Shishkova E & Meyer JG (2021) Peptide Correlation Analysis (PeCorA) Reveals Differential Proteoform Regulation. *J Proteome Res* 20: 1972–1980

Derrien B, Majeran W, Wollman F-A & Vallon O (2009) Multistep Processing of an Insertion Sequence in an Essential Subunit of the Chloroplast ClpP Complex *. *J Biol Chem* 284: 15408–15415

Dix MM, Simon GM & Cravatt BF (2008) Global mapping of the topography and magnitude of proteolytic events in apoptosis. *Cell* 134: 679–691

Dyson HJ & Wright PE (2005) Intrinsically unstructured proteins and their functions. *Nat Rev Mol Cell Biol* 6: 197–208

Elbaum-Garfinkle S, Kim Y, Szczepaniak K, Chen CC-H, Eckmann CR, Myong S & Brangwynne CP (2015) The disordered P granule protein LAF-1 drives phase separation into droplets

with tunable viscosity and dynamics. *Proc Natl Acad Sci* 112: 7189–7194
Eng JK, Jahan TA & Hoopmann MR (2013) Comet: an open-source MS/MS sequence database search tool. *Proteomics* 13: 22–24
Etchison D, Milburn SC, Edery I, Sonenberg N & Hershey JW (1982) Inhibition of HeLa cell protein synthesis following poliovirus infection correlates with the proteolysis of a 220,000-dalton polypeptide associated with eucaryotic initiation factor 3 and a cap binding protein complex. *J Biol Chem* 257: 14806–14810
Follit JA, Li L, Vucica Y & Pazour GJ (2010) The cytoplasmic tail of fibrocystin contains a ciliary targeting sequence. *J Cell Biol* 188: 21–28
Gevaert K, Goethals M, Martens L, Van Damme J, Staes A, Thomas GR & Vandekerckhove J (2003) Exploring proteomes and analyzing protein processing by mass spectrometric identification of sorted N-terminal peptides. *Nat Biotechnol* 21: 566–569
Gibson DG, Young L, Chuang R-Y, Venter JC, Hutchison CA & Smith HO (2009) Enzymatic assembly of DNA molecules up to several hundred kilobases. *Nat Methods* 6: 343–345
Gordon WR, Vardar-Ulu D, Histen G, Sanchez-Irizarry C, Aster JC & Blacklow SC (2007) Structural basis for autoinhibition of Notch. *Nat Struct Mol Biol* 14: 295–300
Guillén-Boixet J, Kopach A, Holehouse AS, Wittmann S, Jahnel M, Schlüßler R, Kim K, Trussina IREA, Wang J, Mateju D, *et al* (2020) RNA-Induced Conformational Switching and Clustering of G3BP Drive Stress Granule Assembly by Condensation. *Cell* 181: 346-361.e17
Havugimana PC, Hart GT, Nepusz T, Yang H, Turinsky AL, Li Z, Wang PI, Boutz DR, Fong V, Phanse S, *et al* (2012) A census of human soluble protein complexes. *Cell* 150: 1068–1081
He S, Chou H-T, Matthies D, Wunder T, Meyer MT, Atkinson N, Martinez-Sanchez A, Jeffrey PD, Port SA, Patena W, *et al* (2020) The structural basis of Rubisco phase separation in the pyrenoid. *Nat Plants* 6: 1480–1490
Henikoff S, Sloan JS & Kelly JD (1983) A Drosophila metabolic gene transcript is alternatively processed. *Cell* 34: 405–414
Hiesberger T, Gourley E, Erickson A, Koulen P, Ward CJ, Masyuk TV, Larusso NF, Harris PC & Igarashi P (2006) Proteolytic cleavage and nuclear translocation of fibrocystin is regulated by intracellular Ca2+ and activation of protein kinase C. *J Biol Chem* 281: 34357–34364
Ivanov P, Kedersha N & Anderson P (2019) Stress Granules and Processing Bodies in Translational Control. *Cold Spring Harb Perspect Biol* 11: a032813
Jagdeo JM, Dufour A, Fung G, Luo H, Kleifeld O, Overall CM & Jan E (2015) Heterogeneous Nuclear Ribonucleoprotein M Facilitates Enterovirus Infection. *J Virol* 89: 7064–7078
Kaimori J, Nagasawa Y, Menezes LF, Garcia-Gonzalez MA, Deng J, Imai E, Onuchic LF, Guay-Woodford LM & Germino GG (2007) Polyductin undergoes notch-like processing and regulated release from primary cilia. *Hum Mol Genet* 16: 942–956
Käll L, Krogh A & Sonnhammer ELL (2007) Advantages of combined transmembrane topology and signal peptide prediction—the Phobius web server. *Nucleic Acids Res* 35: W429–W432
Kan JL & Moran RG (1995) Analysis of a mouse gene encoding three steps of purine synthesis reveals use of an intronic polyadenylation signal without alternative exon usage. *J Biol Chem* 270: 1823–1832
Keul ND, Oruganty K, Schaper Bergman ET, Beattie NR, McDonald WE, Kadirvelraj R, Gross ML, Phillips RS, Harvey SC & Wood ZA (2018) The entropic force generated by intrinsically disordered segments tunes protein function. *Nature* 563: 584–588
Kim S & Pevzner PA (2014) MS-GF+ makes progress towards a universal database search tool for proteomics. *Nat Commun* 5: 5277
Kopan R & Ilagan MaXG (2009) The Canonical Notch Signaling Pathway: Unfolding the

Activation Mechanism. *Cell* 137: 216–233
Kristensen AR, Gsponer J & Foster LJ (2012) A high-throughput approach for measuring temporal changes in the interactome. *Nat Methods* 9: 907–9
Kwon T, Choi H, Vogel C, Nesvizhskii AI & Marcotte EM (2011) MSblender: A probabilistic approach for integrating peptide identifications from multiple database search engines. *J Proteome Res* 10: 2949–2958
Lamesch P, Berardini TZ, Li D, Swarbreck D, Wilks C, Sasidharan R, Muller R, Dreher K, Alexander DL, Garcia-Hernandez M, *et al* (2012) The Arabidopsis Information Resource (TAIR): improved gene annotation and new tools. *Nucleic Acids Res* 40: D1202-1210
Liebeskind BJ, Young RL, Halling DB, Aldrich RW & Marcotte EM (2020) Mapping Functional Protein Neighborhoods in the Mouse Brain. *bioRxiv*: 2020.01.26.920447
Lin Y, Currie SL & Rosen MK (2017) Intrinsically disordered sequences enable modulation of protein phase separation through distributed tyrosine motifs. *J Biol Chem* 292: 19110–19120
Liu J, Perumal NB, Oldfield CJ, Su EW, Uversky VN & Dunker AK (2006) Intrinsic Disorder in Transcription Factors. *Biochemistry* 45: 6873–6888
Liu Y, Gonzàlez-Porta M, Santos S, Brazma A, Marioni JC, Aebersold R, Venkitaraman AR & Wickramasinghe VO (2017) Impact of Alternative Splicing on the Human Proteome. *Cell Rep* 20: 1229–1241
Lo W-S, Gardiner E, Xu Z, Lau C-F, Wang F, Zhou JJ, Mendlein JD, Nangle LA, Chiang KP, Yang X-L, *et al* (2014) Human tRNA synthetase catalytic nulls with diverse functions. *Science* 345: 328–332
Löffler J & Huber G (1992) β-Amyloid Precursor Protein Isoforms in Various Rat Brain Regions and During Brain Development. *J Neurochem* 59: 1316–1324
Lu P, Vogel C, Wang R, Yao X & Marcotte EM (2007) Absolute protein expression profiling estimates the relative contributions of transcriptional and translational regulation. *Nat Biotechnol* 25: 117–124
Mallam AL, Sae-Lee W, Schaub JM, Tu F, Battenhouse A, Jang YJ, Kim J, Wallingford JB, Finkelstein IJ, Marcotte EM, *et al* (2019) Systematic Discovery of Endogenous Human Ribonucleoprotein Complexes. *Cell Rep* 29: 1351-1368.e5
Mallick P, Schirle M, Chen SS, Flory MR, Lee H, Martin D, Ranish J, Raught B, Schmitt R, Werner T, *et al* (2007) Computational prediction of proteotypic peptides for quantitative proteomics. *Nat Biotechnol* 25: 125–31
Mathieu-Rivet E, Scholz M, Arias C, Dardelle F, Schulze S, Le Mauff F, Teo G, Hochmal AK, Blanco-Rivero A, Loutelier-Bourhis C, *et al* (2013) Exploring the N-glycosylation pathway in Chlamydomonas reinhardtii unravels novel complex structures. *Mol Cell Proteomics MCP* 12: 3160–3183
McBride Z, Chen D, Lee Y, Aryal UK, Xie J & Szymanski DB (2019) A Label-Free Mass Spectrometry Method to Predict Endogenous Protein Complex Composition. *Mol Cell Proteomics*: mcp.RA119.001400
McWhite CD, Papoulas O, Drew K, Cox RM, June V, Dong OX, Kwon T, Wan C, Salmi ML, Roux SJ, *et al* (2020) A Pan-plant Protein Complex Map Reveals Deep Conservation and Novel Assemblies. *Cell* 181: 460-474.e14
McWhite CD, Papoulas O, Drew K, Dang V, Leggere JC, Sae-Lee W & Marcotte EM (2021) Co-fractionation/mass spectrometry to identify protein complexes. *STAR Protoc* 2: 100370
Neurath H (1980) Limited proteolysis, protein folding and physiological regulation. In *Protein Folding* pp 501–504. Amsterdam-New York: Elsevier/North Holland Biomedical Press
Neurath H & Walsh KA (1976) Role of proteolytic enzymes in biological regulation (a review). *Proc Natl Acad Sci* 73: 3825–3832
Okumoto K, Kametani Y & Fujiki Y (2011) Two proteases, trypsin domain-containing 1 (Tysnd1)

and peroxisomal lon protease (PsLon), cooperatively regulate fatty acid β-oxidation in peroxisomal matrix. *J Biol Chem* 286: 44367–44379
Pang CNI, Ballouz S, Weissberger D, Thibaut LM, Hamey JJ, Gillis J, Wilkins MR & Hart-Smith G (2020) Analytical Guidelines for co-fractionation Mass Spectrometry Obtained through Global Profiling of Gold Standard Saccharomyces cerevisiae Protein Complexes. *Mol Cell Proteomics MCP* 19: 1876–1895
Perez-Riverol Y, Csordas A, Bai J, Bernal-Llinares M, Hewapathirana S, Kundu DJ, Inuganti A, Griss J, Mayer G, Eisenacher M, *et al* (2019) The PRIDE database and related tools and resources in 2019: improving support for quantification data. *Nucleic Acids Res* 47: D442–D450
Pourhaghighi R, Ash PEA, Phanse S, Goebels F, Hu LZM, Chen S, Zhang Y, Wierbowski SD, Boudeau S, Moutaoufik MT, *et al* (2020) BraInMap Elucidates the Macromolecular Connectivity Landscape of Mammalian Brain. *Cell Syst* 10: 333-350.e14
Qeli E, Omasits U, Goetze S, Stekhoven DJ, Frey JE, Basler K, Wollscheid B, Brunner E & Ahrens CH (2014) Improved prediction of peptide detectability for targeted proteomics using a rank-based algorithm and organism-specific data. *J Proteomics* 108: 269–283
Richardson RT, Batova IN, Widgren EE, Zheng LX, Whitfield M, Marzluff WF & O'Rand MG (2000) Characterization of the histone H1-binding protein, NASP, as a cell cycle-regulated somatic protein. *J Biol Chem* 275: 30378–30386
Saeed M, Kapell S, Hertz NT, Wu X, Bell K, Ashbrook AW, Mark MT, Zebroski HA, Neal ML, Flodström-Tullberg M, *et al* (2020) Defining the proteolytic landscape during enterovirus infection. *PLOS Pathog* 16: e1008927
Sae-Lee W, McCafferty CL, Verbeke EJ, Havugimana PC, Papoulas O, McWhite CD, Houser JR, Vanuytsel K, Murphy GJ, Drew K, *et al* (2021) The protein organization of a red blood cell. 2021.12.10.472004 doi:10.1101/2021.12.10.472004 [PREPRINT]
Sae-Lee W, McCafferty CL, Verbeke EJ, Havugimana PC, Papoulas O, McWhite CD, Houser JR, Vanuytsel K, Murphy GJ, Drew K, *et al* (2022) The protein organization of a red blood cell. *Cell Rep* 40: 111103
Sanders DW, Kedersha N, Lee DSW, Strom AR, Drake V, Riback JA, Bracha D, Eeftens JM, Iwanicki A, Wang A, *et al* (2020) Competing protein-RNA interaction networks control multiphase intracellular organization. *Cell* 181: 306-324.e28
Shortreed MR, Frey BL, Scalf M, Knoener RA, Cesnik AJ & Smith LM (2016) Elucidating Proteoform Families from Proteoform Intact-Mass and Lysine-Count Measurements. *J Proteome Res* 15: 1213–1221
Skinnider MA & Foster LJ (2021) Meta-analysis defines principles for the design and analysis of co-fractionation mass spectrometry experiments. *Nat Methods* 18: 806–815
Skinnider MA, Scott NE, Prudova A, Kerr CH, Stoynov N, Stacey RG, Chan QWT, Rattray D, Gsponer J & Foster LJ (2021) An atlas of protein-protein interactions across mouse tissues. *Cell* 184: 4073-4089.e17
Smith LM & Kelleher NL (2013) Proteoform: a single term describing protein complexity. *Nat Methods* 10: 186–187
Staes A, Impens F, Van Damme P, Ruttens B, Goethals M, Demol H, Timmerman E, Vandekerckhove J & Gevaert K (2011) Selecting protein N-terminal peptides by combined fractional diagonal chromatography. *Nat Protoc* 6: 1130–1141
Suskiewicz MJ, Sussman JL, Silman I & Shaul Y (2011) Context-dependent resistance to proteolysis of intrinsically disordered proteins. *Protein Sci Publ Protein Soc* 20: 1285–1297
Takano E, Kitahara A, Sasaki T, Kannagi R & Murachi T (1986) Two different molecular species of pig calpastatin. Structural and functional relationship between 107 kDa and 68 kDa molecules. *Biochem J* 235: 97–102
Tanco S, Aviles FX, Gevaert K, Lorenzo J & Van Damme P (2017) Identification of

Carboxypeptidase Substrates by C-Terminal COFRADIC. *Methods Mol Biol Clifton NJ* 1574: 115–133
Thul PJ, Åkesson L, Wiking M, Mahdessian D, Geladaki A, Ait Blal H, Alm T, Asplund A, Björk L, Breckels LM, *et al* (2017) A subcellular map of the human proteome. *Science* 356: eaal3321
Tran JC, Zamdborg L, Ahlf DR, Lee JE, Catherman AD, Durbin KR, Tipton JD, Vellaichamy A, Kellie JF, Li M, *et al* (2011) Mapping intact protein isoforms in discovery mode using top-down proteomics. *Nature* 480: 254–258
Tress ML, Abascal F & Valencia A (2017) Alternative Splicing May Not Be the Key to Proteome Complexity. *Trends Biochem Sci* 42: 98–110
Ultsch A, Thrun MC, Hansen-Goos O & Lötsch J (2015) Identification of Molecular Fingerprints in Human Heat Pain Thresholds by Use of an Interactive Mixture Model R Toolbox (AdaptGauss). *Int J Mol Sci* 16: 25897–25911
UniProt Consortium (2019) UniProt: a worldwide hub of protein knowledge. *Nucleic Acids Res* 47: D506–D515
Uversky VN (2013) The most important thing is the tail: Multitudinous functionalities of intrinsically disordered protein termini. *FEBS Lett* 587: 1891–1901
Vagin O, Kraut JA & Sachs G (2009) Role of N-glycosylation in trafficking of apical membrane proteins in epithelia. *Am J Physiol - Ren Physiol* 296: F459–F469
Van Damme P, Gawron D, Van Criekinge W & Menschaert G (2014) N-terminal proteomics and ribosome profiling provide a comprehensive view of the alternative translation initiation landscape in mice and men. *Mol Cell Proteomics MCP* 13: 1245–1261
Wan C, Borgeson B, Phanse S, Tu F, Drew K, Clark G, Xiong X, Kagan O, Kwan J, Bezginov A, *et al* (2015) Panorama of ancient metazoan macromolecular complexes. *Nature* 525: 339–344
Yang P, Mathieu C, Kolaitis R-M, Zhang P, Messing J, Yurtsever U, Yang Z, Wu J, Li Y, Pan Q, *et al* (2020) G3BP1 Is a Tunable Switch that Triggers Phase Separation to Assemble Stress Granules. *Cell* 181: 325-345.e28
You K, Huang Q, Yu C, Shen B, Sevilla C, Shi M, Hermjakob H, Chen Y & Li T (2020) PhaSepDB: a database of liquid–liquid phase separation related proteins. *Nucleic Acids Res* 48: D354–D359
Zhang Y, Yao L, Xu X, Han H, Li P, Zou D, Li X, Zheng L, Cheng L, Shen Y, *et al* (2018) Enterovirus 71 inhibits cytoplasmic stress granule formation during the late stage of infection. *Virus Res* 255: 55–67

**Supporting Files**

- **Supplemental File 1**: Description of individual fractionation experiments and deposition identifiers
- **Supplemental File 2**: Curated candidate alternative proteoforms with estimated amino acid boundary positions from the peptide data

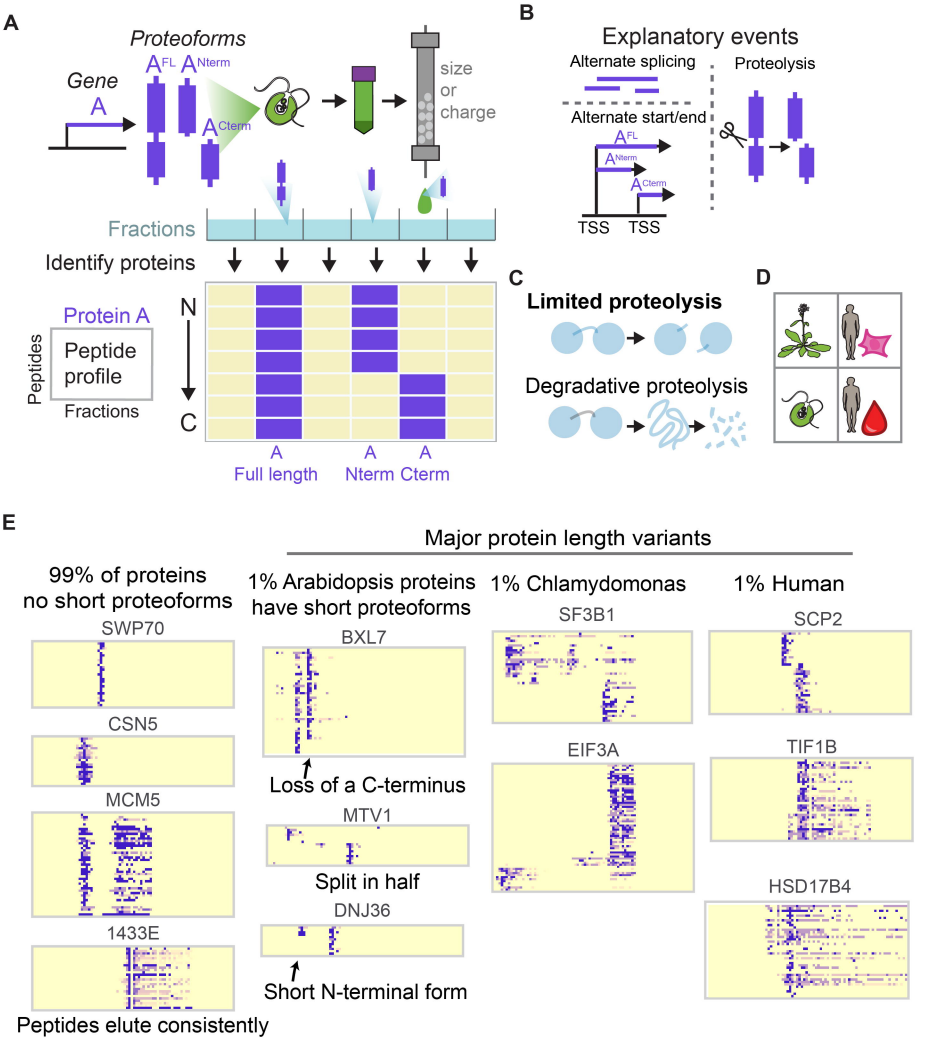
A
Proteoforms
Gene
A
A FL
A Nterm
A Cterm
size
or
charge
Fractions
Identify proteins
Protein A
Peptide
profile
Peptides
Fractions
N
C
A
Full length
A
Nterm
A
Cterm
B
Explanatory events
Alternate splicing
Proteolysis
Alternate start/end
A FL
A Nterm
A Cterm
TSS
TSS
C
Limited proteolysis
Degradative proteolysis
D
E
Major protein length variants
99% of proteins
no short proteoforms
1% Arabidopsis proteins
have short proteoforms
1% Chlamydomonas
1% Human
SWP70
CSN5
MCM5
1433E
Peptides elute consistently
BXL7
Loss of a C-terminus
MTV1
Split in half
DNJ36
Short N-terminal form
SF3B1
EIF3A
SCP2
TIF1B
HSD17B4

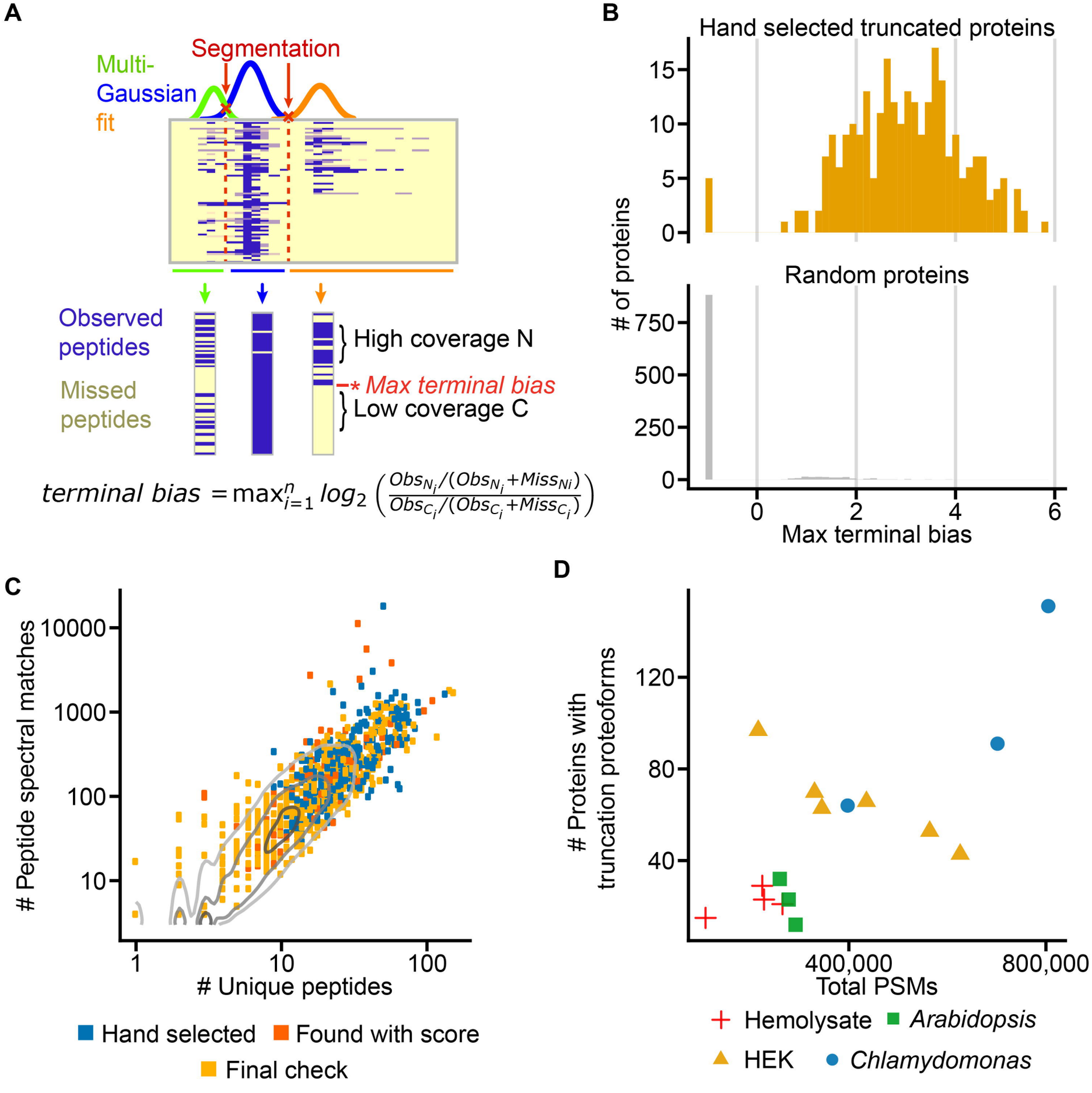
A
Segmentation
Multi-
Gaussian
fit
Observed
peptides
Missed
peptides
High coverage N
Max terminal bias
Low coverage C
$terminal\ bias = \max_{i=1}^{n} log_2 \left( \frac{Obs_{N_i}/(Obs_{N_i}+Miss_{Ni})}{Obs_{C_i}/(Obs_{C_i}+Miss_{C_i})} \right)$
B
Hand selected truncated proteins
Random proteins
# of proteins
Max terminal bias
C
# Peptide spectral matches
# Unique peptides
Hand selected
Found with score
Final check
D
# Proteins with
truncation proteoforms
Total PSMs
Hemolysate
Arabidopsis
HEK
Chlamydomonas

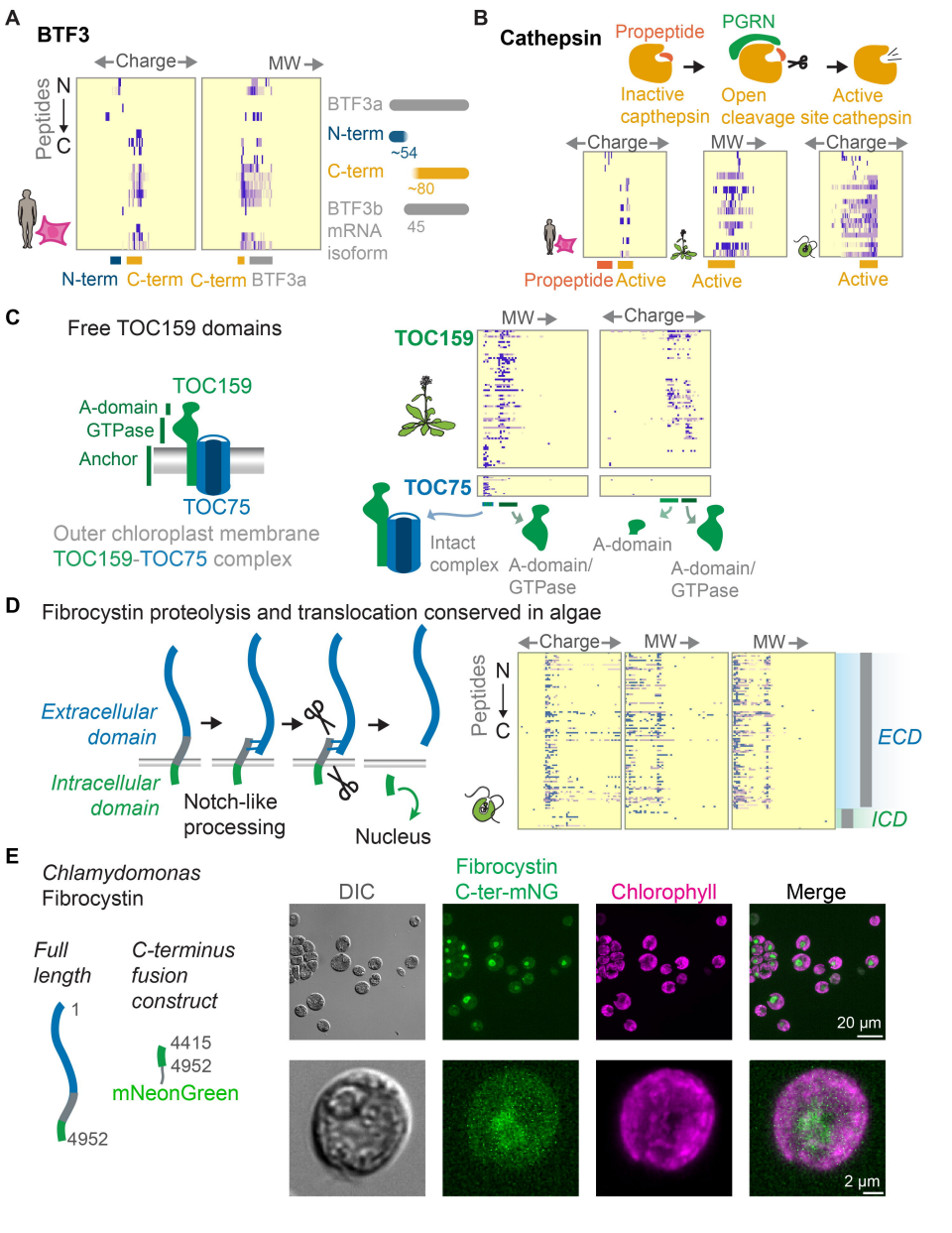
A
BTF3
Charge
MW
Peptides
N
C
BTF3a
N-term
~54
C-term
~80
BTF3b
mRNA
isoform
45
N-term
C-term
C-term
BTF3a
B
Cathepsin
Propeptide
PGRN
Inactive
capthepsin
Open
cleavage site
Active
cathepsin
Charge
MW
Charge
Propeptide
Active
Active
Active
C
Free TOC159 domains
TOC159
A-domain
GTPase
Anchor
TOC75
Outer chloroplast membrane
TOC159-TOC75 complex
MW
Charge
TOC159
TOC75
Intact
complex
A-domain/
GTPase
A-domain
A-domain/
GTPase
D
Fibrocystin proteolysis and translocation conserved in algae
Extracellular
domain
Intracellular
domain
Notch-like
processing
Nucleus
Charge
MW
MW
Peptides
N
C
ECD
ICD
E
Chlamydomonas
Fibrocystin
Full
length
C-terminus
fusion
construct
1
4415
4952
mNeonGreen
4952
DIC
Fibrocystin
C-ter-mNG
Chlorophyll
Merge
20 µm
2 µm

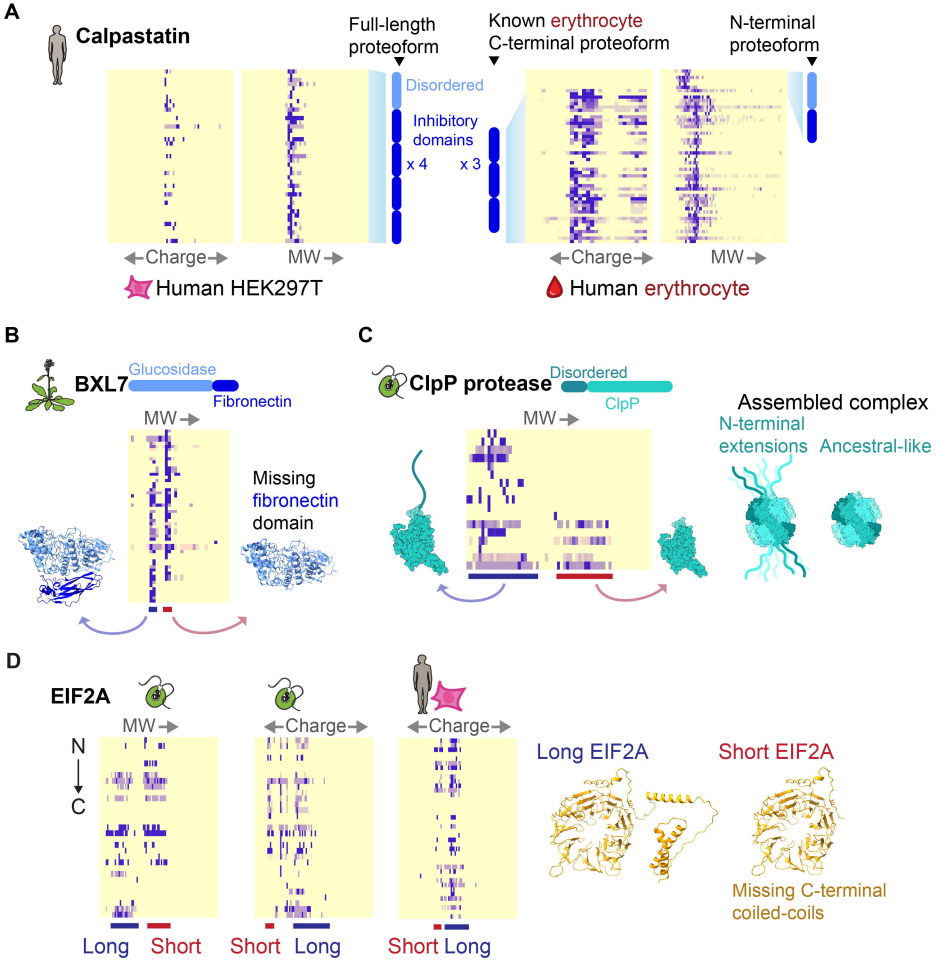
A
Calpastatin
Full-length proteoform
Known erythrocyte C-terminal proteoform
N-terminal proteoform
Disordered
Inhibitory domains
x 4
x 3
Charge
MW
Charge
MW
Human HEK297T
Human erythrocyte
B
BXL7
Glucosidase
Fibronectin
MW
Missing fibronectin domain
C
ClpP protease
Disordered
ClpP
MW
Assembled complex
N-terminal extensions
Ancestral-like
D
EIF2A
MW
Charge
Charge
N
C
Long
Short
Short
Long
Short
Long
Long EIF2A
Short EIF2A
Missing C-terminal coiled-coils

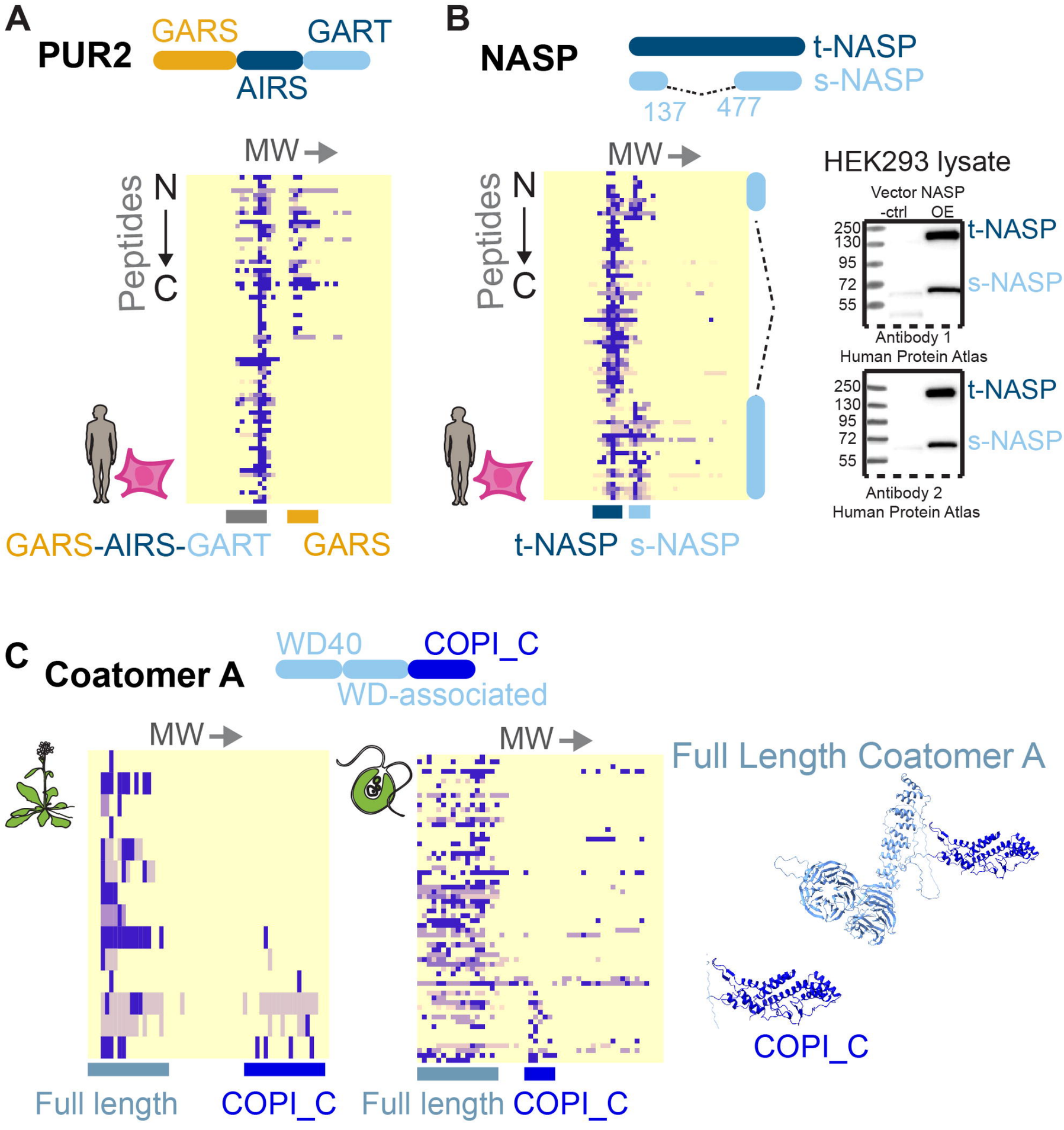
A
PUR2
GARS
GART
AIRS
MW
Peptides
N
C
GARS-AIRS-GART
GARS
B
NASP
t-NASP
s-NASP
137
477
MW
Peptides
N
C
t-NASP
s-NASP
HEK293 lysate
Vector NASP
-ctrl
OE
250
130
95
72
55
t-NASP
s-NASP
Antibody 1
Human Protein Atlas
250
130
95
72
55
t-NASP
s-NASP
Antibody 2
Human Protein Atlas
C
Coatomer A
WD40
COPI_C
WD-associated
MW
MW
Full Length Coatomer A
COPI_C
Full length
COPI_C
Full length
COPI_C

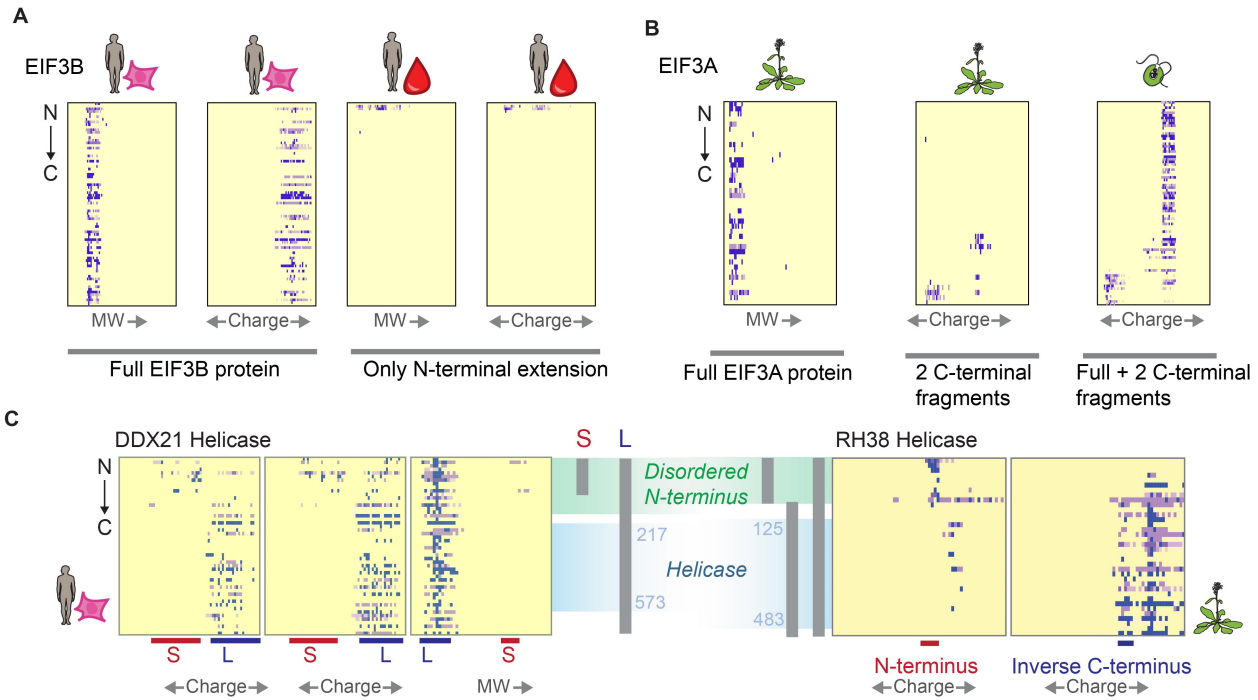


D **Common categories of candidate truncated proteins**

| Phase separating | Helicase | Translation |
|---|---|---|
| | | **eIF2A** |
| **NPM1** | DDX3x | **eIF2S2** |
| **NUP98*** | **DDX6*** | eIF2B3 |
| ATXN2 | **DDX17** | eIF2P |
| EIF4G1* | **DDX42** | **eIF4B** |
| EIF4G2* | **DDX46** | eIF3A |
| UBAP2L | DDX50 | **eIF5B*** |
| KPNB1 | **DHX9*** | |
| **G3BP1*** | | |
| **DDX21** | | |
| **HNRPM*** | | |
| SRRM2 | SRRM domain | |
| TCOF1 | | |
| ACIN1 | | |

*terminus known cleaved by enterovirus

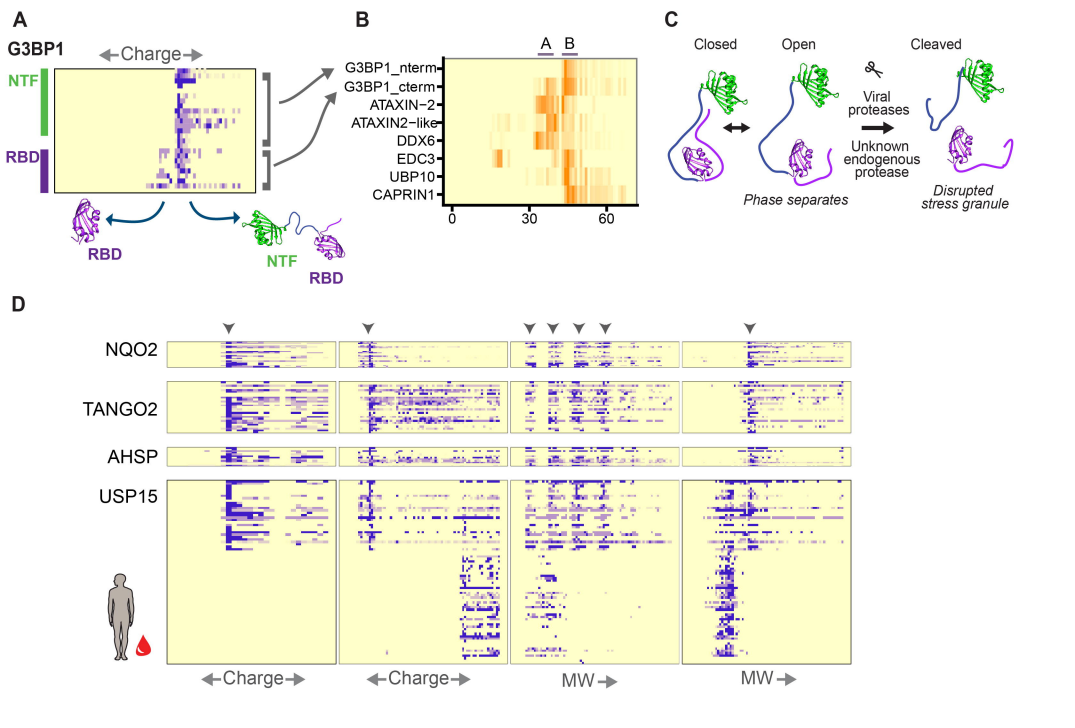
A
G3BP1
Charge
NTF
RBD
RBD
NTF
RBD
B
A
B
G3BP1_nterm
G3BP1_cterm
ATAXIN−2
ATAXIN2−like
DDX6
EDC3
UBP10
CAPRIN1
0
30
60
C
Closed
Open
Cleaved
Viral proteases
Unknown endogenous protease
Phase separates
Disrupted stress granule
D
NQO2
TANGO2
AHSP
USP15
Charge
Charge
MW
MW

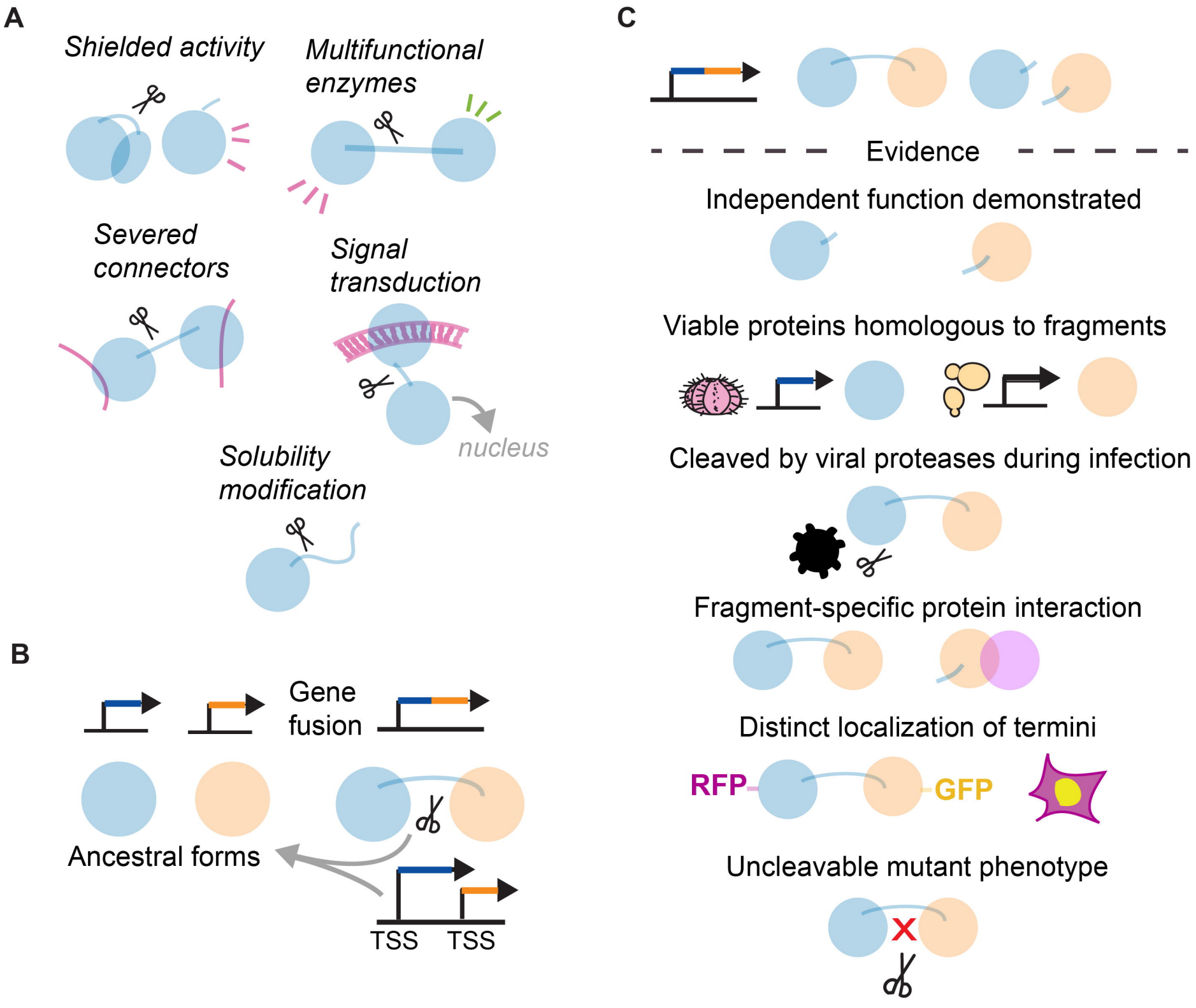
A
Shielded activity
Multifunctional enzymes
Severed connectors
Signal transduction
nucleus
Solubility modification
B
Gene fusion
Ancestral forms
TSS
TSS
C
Evidence
Independent function demonstrated
Viable proteins homologous to fragments
Cleaved by viral proteases during infection
Fragment-specific protein interaction
Distinct localization of termini
RFP
GFP
Uncleavable mutant phenotype
X